foods

MDPI

Article

Gut Microbiome Modulation by Fermented Rice Bran and Tryptamine Before and After DSS-Induced Colitis

Tafriha E Tasdika [1,2,†], Jahidul Islam [3,4,*,†], Md Alauddin [5], Afifah Zahra Agista [1,6], Mutsumi Furukawa [4], Fahmida Siddika [7], Hsin-Jung Ho [1,8], Yusuke Ohsaki [1,6], Ya-Ling Chen [9], Wan-Chun Chiu [9], Chiu-Li Yeh [9], Tomonori Nochi [4], Suh-Ching Yang [9], Md. Zakir Hossain Howlader [10], Yearul Kabir [5] and Hitoshi Shirakawa [1,6,*]

1 Laboratory of Nutrition, Graduate School of Agricultural Science, Tohoku University, Sendai 980-8572, Japan; tafriha16@gmail.com (T.E.T.); agista@g-mail.tohoku-university.jp (A.Z.A.); hjho@tohoku.ac.jp (H.-J.H.); yusuke.ohsaki.a4@tohoku.ac.jp (Y.O.)
2 Department of Biochemistry and Molecular Biology, Primeasia University, Dhaka 1213, Bangladesh
3 Laboratory of Animal Data Science & Innovation, Division of Animal Immunology and Omics, International Education and Research Center for Food Agricultural Immunology, Graduate School of Agricultural Science, Tohoku University, Sendai 980-8572, Japan
4 Laboratory of Animal Functional Morphology, Graduate School of Agricultural Science, Tohoku University, Sendai 980-8572, Japan; mutsumi.furukawa.c4@tohoku.ac.jp (M.F.); tomonori.nochi.a5@tohoku.ac.jp (T.N.)
5 Department of Biochemistry and Molecular Biology, Jashore University of Science and Technology, Jashore 7408, Bangladesh; mdalauddin_nft@just.edu.bd (M.A.); ykabir@yahoo.com (Y.K.)
6 Food and Health Evaluation Unit, International Education and Research Center for Food Agricultural Immunology, Graduate School of Agricultural Science, Tohoku University, Sendai 980-8572, Japan
7 Department of Pathology, Tairunnessa Memorial Medical College, Gazipur 1704, Bangladesh; fahmidasiddika@gmail.com
8 Institute for Excellence in Higher Education, Tohoku University, Sendai 980-8576, Japan
9 School of Nutrition and Health Sciences, College of Nutrition, Taipei Medical University, Taipei 11031, Taiwan; ylchen01@tmu.edu.tw (Y.-L.C.); wanchun@tmu.edu.tw (W.-C.C.); clyeh@tmu.edu.tw (C.-L.Y.); sokei@tmu.edu.tw (S.-C.Y.)
10 Laboratory of Nutrition and Health Research, Department of Biochemistry and Molecular Biology, University of Dhaka, Dhaka 1000, Bangladesh; hhzakir@du.ac.bd
* Correspondence: islam.jahidul.a5@tohoku.ac.jp (J.I.); shirakah@tohoku.ac.jp (H.S.)
† These authors contributed equally to this work.

Abstract

Fermented rice bran (FRB) attenuates experimental colitis, but its effects on gut microbiome remodeling before disease onset and whether these changes contribute to protection against colitis remain unclear. Furthermore, the contribution of tryptamine (TRY), a fermentation-associated metabolite, to these effects has not been established. We compared FRB, TRY, and their combination (FT) before and after dextran sulfate sodium (DSS)-induced colitis. Female C57BL/6N mice (n = 8/group) received control, FRB (10%), TRY (0.1%), or FT diets for 1 week before DSS administration. Fecal and cecal microbiota were analyzed by 16S rRNA gene amplicon sequencing (n = 6/group), alongside clinical, histopathological, host-response assessments. Before DSS exposure, FRB and FT significantly altered microbial community structure (PERMANOVA, p = 0.004), whereas TRY induced modest changes. FRB enriched *Duncaniella*, *Prevotella*, and *Alistipes_A_871400*; FT enriched *Nanosynococcus*, *UMGS1994*, and *UBA3263*. Following DSS exposure, FRB-containing diets attenuated dysbiosis and showed higher proportions of shared PICRUSt2-predicted pathways between pre-colitis fecal and post-colitis cecal microbiota (FRB, 93.5%; FT, 94.4%) compared with control diet with DSS (88.1%), whereas TRY showed 90.4% continuity. Overall, FRB preconditioned the gut microbiota before inflammatory challenge and promoted microbial resilience, whereas TRY attenuated intestinal injury without comparable microbiome remodeling, suggesting distinct mechanisms underlying their effects.

Check for updates

Academic Editor: Baojun Xu

Received: 27 September 2026
Revised: 29 October 2026
Accepted: 12 November 2026
Published: 18 November 2026

Copyright: © 2026 by the authors. Licensee MDPI, Basel, Switzerland. This article is an open access article distributed under the terms and conditions of the Creative Commons Attribution (CC BY) license.

Keywords: fermented rice bran; tryptamine; microbiome resilience; DSS-induced colitis; dietary preconditioning; tryptophan metabolism; PICRUSt2

1. Introduction

Inflammatory bowel disease (IBD) is a group of chronic, relapsing inflammatory disorders of the gastrointestinal tract and is broadly classified into two major forms: ulcerative colitis and Crohn's disease [1]. IBD is characterized by impaired intestinal barrier integrity, dysregulated mucosal immune responses, and alterations in the gut microbial ecosystem [1,2]. According to the Global Burden of Disease 2021 study, approximately 3.83 million individuals were living with IBD worldwide, with an estimated 375,140 new cases and 42,423 associated deaths in 2021. The global age-standardized incidence rate was approximately 4.4 cases per 100,000 [3]. The rising global incidence of IBD highlights the important contribution of environmental and dietary factors beyond genetic and geographic influences [4]. In particular, dietary factors may play an important role by influencing the composition and function of the gut microbiota, which, in turn, contributes to intestinal homeostasis through interactions with epithelial and immune cells and the production of bioactive metabolites. Therefore, dietary modulation of the gut microbiota has emerged as a potential strategy to support intestinal health, especially in conditions associated with IBD development [2,5,6]. Biological sex can also influence gut microbiota composition, mucosal immune responses, and susceptibility to intestinal inflammation [7]. Accordingly, female mice were used in the present study to maintain a consistent sex background across experimental groups.

Rice bran is an abundant by-product of rice processing and a rich source of dietary fiber and bioactive compounds. It is demonstrated that dietary fermented rice bran (FRB) attenuates dextran sodium sulfate (DSS)-induced colitis in mice, reducing mucosal injury, inflammatory responses, and pro-inflammatory cytokine expression while influencing short-chain fatty acid (SCFA) production and intestinal barrier-associated responses [5]. Fermentation enhances the functional potential of rice bran by releasing and generating bioactive compounds and generating microbial metabolites with increased inaccessibility and biological activity, providing the rationale for using FRB rather than rice bran itself [8,9]. FRB supplementation has also been shown to promote intestinal recovery and suppress fibrosis following DSS-induced inflammation, accompanied by increased expression of anti-inflammatory cytokines, tight-junction-related molecules, and antimicrobial proteins [10]. More recently, FRB-mediated protection against acute DSS-induced colitis has been associated with modulation of intestinal aryl hydrocarbon receptor (AHR) expression, type 3 innate lymphoid cells (ILC3s), and the fecal microbiota [6].

However, previous studies, including our own, have primarily investigated the protective effects of FRB and associated microbial changes during or after intestinal inflammation [5,6,10–12]. Whether FRB induces microbial community restructuring before inflammatory onset is insufficiently understood. Furthermore, it is unclear whether post-DSS microbial differences reflect pre-existing dietary modulation of the gut microbiota or arise predominantly because of differences in disease severity. Addressing this distinction is important for understanding the potential role of dietary microbiota preconditioning in intestinal resilience.

Microbial metabolites provide an important functional link between diet, the gut microbiota, and host physiology. Tryptophan metabolism is of particular interest because intestinal microorganisms transform dietary tryptophan into diverse bioactive metabolites capable of interacting with epithelial and immune signaling pathways [13,14]. Tryptamine

(TRY) is an aromatic monoamine produced by decarboxylation of tryptophan through gut microbiota *Clostridium sporogenes* and *Ruminococcus gnavus* [15] and can originate from commonly consumed fruits and vegetables as dietary sources [16]. Importantly, fermentation of rice bran markedly increases its TRY content and FRB supplementation increases TRY availability in the host [17], suggesting that this fermentation-derived metabolite may contribute to the functional and potential postbiotic effects of FRB.

In the gastrointestinal tract, bacterial TRY activates epithelial serotonin receptor 4 (5-HT4R), promoting colonic ion and fluid secretion and influencing gastrointestinal transit [18]. Beyond these physiological effects, microbial tryptophan-derived metabolites have been implicated in intestinal immune regulation through AHR-associated signaling, which can promote IL-22-mediated epithelial protection and mucosal homeostasis [19]. However, these immunomodulatory effects are metabolite-specific, and direct involvement of TRY in this pathway remains to be established. Nevertheless, the extent to which TRY contributes to the microbiota-modulating and protective effects of FRB during intestinal inflammation remains unclear. Although FRB naturally contains fermentation-derived TRY, the specific contribution of this metabolite within the complex FRB matrix has not been fully established. This knowledge gap provides a rationale for examining TRY independently and in combination with FRB. TRY supplementation can determine whether direct dietary exposure to a defined tryptophan-derived metabolite modifies the intestinal microbial ecosystem or the host response to DSS-induced injury. In contrast, a combination of both FRB and TRY supplementation can reveal whether exogenous TRY enhances, reproduces, or modifies the effects of an FRB-conditioned intestinal environment. Importantly, such comparisons can help determine whether the biological effects of FRB are associated with broad microbial and metabolic remodeling rather than with the action of a single metabolite.

Therefore, the present study investigated the effects of FRB, TRY, and their combination (FT) on the gut microbiota before and after DSS-induced colitis. Fecal microbiota was characterized at baseline and after one week of dietary supplementation before DSS exposure to determine whether these interventions induced early microbial remodeling, together with intestinal and host responses. Post-DSS cecal microbiota was subsequently examined to evaluate microbial responses to inflammatory challenges. Unlike previous studies, the present investigation integrates longitudinal sampling, direct comparison of the complex FRB matrix with TRY supplementation, reference-based assessment of microbial dysbiosis, and evaluation of predicted microbial functional continuity between pre-colitis fecal and post-colitis cecal communities.

Finally, we hypothesized that FRB preconditions the gut microbiota before inflammatory challenge, thereby promoting microbial resilience during DSS-induced colitis, and that these protective effects may be augmented by TRY supplementation. TRY supplementation was examined to determine whether a defined tryptophan-derived metabolite could reproduce or modify the microbiota preconditioning and host-associated responses of FRB.

2. Materials and Methods

2.1. Materials

The components of the AIN-93M standard diet were purchased from FUJIFILM Wako Pure Chemical Corporation (Osaka, Japan). DSS salt (MW < 50 kDa) was obtained from MP Biomedicals (Solon, OH, USA), tryptamine from Tokyo Chemical Industry (Tokyo, Japan), and the immunoglobulin for ELISA from Bethyl Laboratories (Montgomery, TX, USA).

2.2. Animals

Forty female C57BL/6N mice, aged 9–10 weeks purchased from Japan CLEA (Tokyo, Japan) were used in this study. Female mice were used to maintain a consistent sex background throughout the experiment and reduce potential sex-related variability within the experimental groups [20]. Before the experiment, they had free access to a standard commercial diet (F2 diet, Funabashi Farm, Chiba, Japan). The animals were housed in a specific pathogen-free colony under controlled environmental conditions (temperature: 23 ± 3 °C; relative humidity: 55 ± 10%; 12 h light/dark cycle), with food and water provided *ad libitum*. Mice were housed at a density of two animals per cage, with four cages allocated to each experimental group (n = 8 mice/group; 20 cages in total). All experimental procedures were approved by the Animal Care Committee of Tohoku University and carried out in strict accordance with their guidelines (approved number 2019AgA-011-08), as well as with the Japanese government's animal welfare legislation (2005).

2.3. Preparation of FRB

FRB was prepared from the bran of BRRI dhan84 (BR-84), a zinc-biofortified red-pericarp rice variety developed by the Bangladesh Rice Research Institute (BRRI) for cultivation during the Boro season in Bangladesh. Polished grains of BR-84 contain approximately 27.6 mg/kg zinc, providing a nutritionally distinct substrate for fermentation [21]. Rice bran was collected from BRRI after milling, stabilized at 121 °C for 15 min within 24 h of milling, and subsequently defatted using *n*-hexane at a ratio of 1:3. FRB was produced as previously described [22]. Briefly, a probiotic consortium consisting of rice bran was fermented for 72 h with a probiotic consortium containing *Lactobacillus acidophilus* (2×10^9 CFU), *Lactobacillus delbrueckii* subsp. bulgaricus (1×10^9 CFU), and *Bifidobacterium bifidum* (1×10^9 CFU), at a ratio of 2:1:1 was prepared by suspending 0.5 g of the probiotic blend in 10 mL of sterile water. The consortium was pre-cultured in nutrient broth at 37 °C and 180 rpm for 48 h using a shaking incubator (Biobase BJPS-103B, Biobase Biodustry (Shandong) Co., Ltd., Jinan, China). The resulting inoculum was subsequently used to ferment the defatted rice bran at 37 °C for 72 h under aseptic conditions. The broth pH was 3.8 after 48 h of preculturing. Following fermentation, the resulting FRB was dried at 40–60 °C for 48 h, finely ground, and stored in sterile containers at 4 °C until use. The final FRB preparation had a moisture content of 22.77%. The microbiological quality of the prepared FRB was evaluated by screening for selected bacterial and fungal microorganisms. None of the ten tested microorganisms were detected in the FRB sample (Supplementary Table S1). However, the viability of *Lactobacillus* spp. following heat treatment at 60 °C was not determined. Crude fiber content was determined by proximate analysis, and total phenolic content (TPC) was measured spectrophotometrically using gallic acid as the calibration standard. The FRB preparation contained 33.30% crude fiber and a TPC of 345.03 ± 8.95 mg GAE/g dry weight (mean ± SD, n = 3). Endogenous tryptamine content in FRB was not determined.

2.4. Study Design

Mice were either provided a control diet (AIN93M standard diet for rodents) or the control diet supplemented with 10% (*w*/*w*) FRB, 0.1% TRY (*w*/*w*), and 10% FRB with 0.1% TRY (n = 8/group). The 10% FRB supplementation level was selected based on our previous studies demonstrating its protective effects against DSS-induced colitis [5]. As no established dietary dose of TRY exists for this model, the 0.1% supplementation level was selected as an exploratory dose, informed by our previous study showing that 0.5% dietary tryptophan attenuated DSS-induced colitis [17]. The same TRY concentration was maintained in the FT diet to evaluate its effects in combination with FRB. Experimental diet composition was as illustrated in Supplementary Table S2. Following 7 days of experimental

diet, we added 3% DSS to the drinking water. The 3% DSS concentration was selected based on its established ability to induce intestinal mucosal damage and alterations in gut microbial community composition [23]. The overall experimental follow is shown in Figure 1A. All experimental diets were introduced 7 days prior to the DSS treatment and provided *ad libitum* throughout the study. After a 7-day acclimation period on standard AIN-93M diet, mice were assigned to the respective experimental diets, except for the untreated and DSS-only control groups.

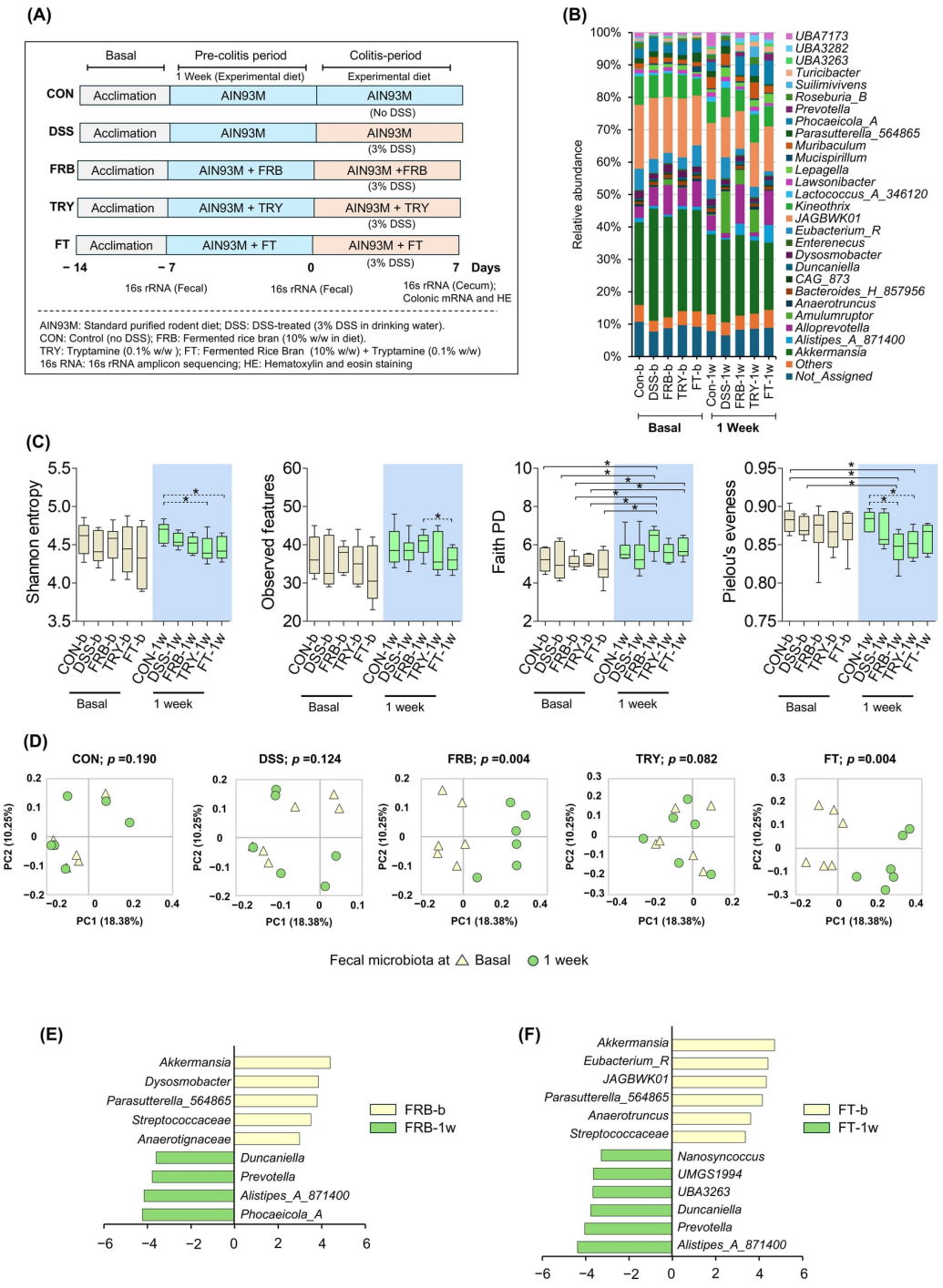


Figure 1. Experimental design, clinical outcomes, and gut microbiota responses to dietary interventions before DSS-induced colitis. Following acclimation, mice received the indicated AIN93M-based diets before DSS administration and throughout the experimental period. (**A**) Schematic representation of experimental design and dietary interventions. White indicates the acclimation period; light

blue indicates the experimental diet period without DSS exposure (and the CON group during the subsequent period); light peach indicates the DSS-treatment period (3% DSS in drinking water). The CON group did not receive DSS. (**B**) Genus-level relative abundance of fecal microbiota at basal (-b) and 1 week (-1w) across all five groups. (**C**) Alpha-diversity indices (Shannon entropy, observed features, Faith's phylogenetic diversity, Pielou's evenness) of fecal microbiota at basal versus 1 week. (**D**) Principal coordinate analysis (PCoA) of fecal microbiota beta diversity comparing basal (triangle) and 1-week (circle) timepoints within each group; PERMANOVA *p*-values shown per group. (**E**,**F**) Linear discriminant analysis effect size (LEfSe) analysis performed using MicrobiomeAnalyst. Data are presented as indicated in each panel. Statistical significance is denoted as * $p < 0.05$. $n = 6$ per group.

Colitis severity was monitored by daily body weight measurements and the disease activity index (DAI). DAI scores were calculated blindly based on stool consistency (diarrhea) and visible gross rectal bleeding is shown in Supplementary Table S3.

2.5. Histopathology

For histopathological analysis, the distal colon tissues (approximately 2–2.5 cm) were excised and gently flushed with cold phosphate-buffered saline (PBS). The tissues were fixed in a 10% neutral-buffered formalin for 24 h, transferred to 70% ethanol and stored at 4 °C, and subsequently processed for paraffin embedding. Fixed tissues were dehydrated through a graded ethanol series (70%, 90%, and 95%; 12 h each), followed by three changes in absolute ethanol (12, 24, and 24 h, respectively). The dehydrated tissues were cleared in three changes in toluene (2–3 h each) and infiltrated with molten paraffin at 60 °C through three successive baths (1 h each). Tissues were then embedded in fresh paraffin using pre-warmed molds, with the sectioning surface facing downward, and cooled on ice-cold water until the blocks solidified.

The paraffin-embedded tissues were sectioned at 5 µm thickness using a microtome (RM2235, Leica Microsystems GmbH, Wetzlar, Germany). Sections were mounted on glass slides, deparaffinized, rehydrated through graded ethanol to water, stained with hematoxylin and eosin (H&E), dehydrated, cleared, and cover slipped with mounting medium. Histological sections were examined using an Olympus CX23 light microscope (Olympus Corporation, Tokyo, Japan) at 10× and 40× magnifications. To evaluate the degree of colitis, colonic injury was independently assessed by three observers, two of whom were blinded to the treatment groups, using a modified histopathological grading system [10]. The histopathological score was determined by the following parameters: (I) epithelial loss, (II) crypt-cell damage, (III) goblet cell depletion, and (IV) infiltration of inflammatory cells into the mucosa. All four parameters were scored from 0 to 4, where 0 = not observed, 1 = mild, 2 = moderate, 3 = severe, and 4 = massive damage.

2.6. Enzyme-Linked Immunosorbent Assay (ELISA)

Plasma IgA concentrations were quantified by an indirect enzyme-linked immunosorbent assay (ELISA) as previously described with modifications [24]. Briefly, 96-well plates were coated with goat anti-mouse IgA antibody and anti-mouse IgG Fc-Fragment antibody. Diluted plasma samples and corresponding IgA and IgG standards were added, the plates were washed with Tris-buffered saline containing Tween 20 (TBS-T) between incubation steps. HRP-conjugated goat anti-mouse IgA and IgG Fc-Fragment antibodies (100 ng/mL) were subsequently added, followed by 3,3′,5,5′-tetramethylbenzidine (TMB) substrate. The reaction was stopped with 0.16 N H_2SO_4, and absorbance was measured at 450 nm. Plasma IgA and IgG concentrations were calculated from the respective standard curves.

2.7. Serum Thiobarbituric Acid Reactive Substances (TBARS) Assay

Plasma lipid peroxidation was assessed by measuring TBARS as an index of malondialdehyde (MDA)-equivalent content, with minor modifications to a previously described method [25]. Briefly, 100 µL of plasma was mixed with 100 µL of 8.1% (*w*/*v*) sodium dodecyl sulfate (SDS), 750 µL of 20% (*v*/*v*) acetic acid (pH 3.5, adjusted with 1 M NaOH), 750 µL of 0.8% (*w*/*v*) thiobarbituric acid (TBA), and 300 µL of purified water, and vortexed. The reaction mixture was heated at 95 °C for 1 h and then immediately cooled on ice. After cooling, 500 µL of purified water and 2.5 mL of *n*-butanol: pyridine (15:1, *v*/*v*) were added, and the mixture was vortexed for 30s and centrifuged at 3000 rpm (4 °C, 10 min). Absorbance of the resulting organic (upper) layer was measured at 532 nm. A standard curve was prepared using 1,1,3,3-tetramethoxypropane (TMP) under identical conditions and used for quantification of TBARS [26].

2.8. mRNA Extraction and Reverse Transcription Quantitative Polymerase Chain Reaction (RT-qPCR)

For RT-qPCR; mRNA was extracted from colon tissue using ISOGEN reagent (Nippon Gene Co., Ltd., Tokyo, Japan) and further purified using NEBNext High Input Poly(A) mRNA Isolation Module (New England Biolabs Inc., Ipswich, MA, USA) according to the manufacturer's instructions. RNA concentration and purity were assessed by UV spectrophotometry using nucleic acid concentration and A260/A280 absorbance ratio, and RNA integrity was verified by agarose gel electrophoresis. The individual nucleic acid concentrations (ng/µL) and A260/A280 ratios are provided in Supplementary Table S4.

The isolated mRNA was used to synthesize cDNA. Briefly, mRNA was mixed with an oligo-dT primer and dNTPs, then incubated at 65 °C for 5 min. The mixture was subsequently combined with 5× First-Strand Buffer containing dithiothreitol (DTT), SuperScript III Reverse Transcriptase (Invitrogen, Carlsbad, CA, USA), and RNaseOUT RNase inhibitor (Invitrogen), followed by reverse transcription at 50 °C. A parallel no-reverse-transcriptase (RT−) control was included for each sample to assess potential genomic DNA contamination.

The resulting cDNA was analyzed by quantitative PCR using a Bio-Rad CFX real-time PCR detection system (Bio-Rad, Hercules, CA, USA). Gene-specific primers and THUNDERBIRD Next SYBR qPCR Mix (TOYOBO Co., Ltd., Osaka, Japan) were used to amplify the target genes in a total reaction volume of 12.5 µL run in duplicate. No-template controls and a standard curve generated from serial dilutions of a representative sample were included on each plate. The amplification specificity was confirmed by melt-curve analysis. Gene expression levels were normalized to eukaryotic elongation factor 1α1 (*Eef1a1*) as the internal standard. The overall primer sequences used for RT-qPCR are provided in the Supplementary Table S5.

2.9. Gut Microbiota Analysis

Fecal samples were collected at baseline and after 7 days of dietary intervention, immediately before DSS administration. Fresh fecal pellets were collected directly from the anus without contact with the cage floor to minimize environmental contamination. Following collection, fecal samples were immediately transferred into collection tubes containing 0.5 mL of guanidinium thiocyanate solution and maintained at room temperature until DNA extraction. At the end of the experimental period, following DSS-induced colitis, approximately 200 mg of cecal contents were collected from each mouse for microbiota analysis.

Fecal and cecal bacterial DNA was extracted using the automated Gene PREP STAR PI-480α sytem (KURABO, Osaka, Japan). The V3–V4 hypervariable region of the bacterial

16S rRNA gene was amplified by PCR using PrimeSTAR HS DNA Polymerase (Takara Bio Inc., Shiga, Japan) and subsequent steps are followed according to a previously established method [27]. The resulting PCR amplicons were sequenced on an Illumina MiSeq platform (Illumina, San Diego, CA, USA) using the MiSeq Reagent Kit v2 (500 cycles). The resulting demultiplexed sequencing were further investigated using the Quantitative Insights into Microbial Ecology 2 (QIIME 2) [28]. The dataset contained a total of 3,024,207 reads, with a mean of 33,602.3 reads per sample (median, 31,779.5; range, 21,611–56,280 reads). Following DADA2 quality filtering, denoising, and chimera removal, 2,762,918 non-chimeric reads (91.36% of the total input reads) were retained for downstream microbiota analyses in QIIME 2. Taxonomic classification of the representative ASV sequences was performed using the Greengenes2 reference database [29]. Microbial α- and β-diversity analyses were performed using the QIIME 2 core-metrics-phylogenetic pipeline at a sampling (rarefaction) depth of 4000 sequences per sample. α-Diversity was assessed using the Shannon entropy, observed features, Faith's phylogenetic diversity (Faith's PD), and Pielou's evenness. β-Diversity was evaluated using UniFrac distance metrics and visualized by principal coordinate analysis (PCoA). For taxonomic composition analyses, QIIME 2-derived taxonomic abundance further analyzed based on family and genus level using MicrobiomeAnalyst [30]. Predicted functional profiles of the gut microbiota were inferred from 16S rRNA gene sequencing data using Phylogenetic Investigation of Communities by Reconstruction of Unobserved States 2 (PICRUSt2) [31].

2.10. Longitudinal Microbiota Dysbiosis Analysis

Longitudinal deviations in the gut microbial community from a healthy reference state were quantified using a Bray–Curtis dissimilarity-based dysbiosis score. The microbial feature table, taxonomic assignments, and sample metadata were integrated in R using the phyloseq package. To standardize sequencing depth, samples were rarefied to the minimum sequencing depth and converted to relative abundances. A healthy reference microbiota was defined from basal samples of untreated control mice maintained on the AIN-93M diet without DSS exposure. The dysbiosis score for each sample was subsequently calculated as the Bray–Curtis dissimilarity between its relative-abundance profile and the healthy reference profile using the vegan package. Accordingly, values approaching 0 indicate greater similarity to the healthy reference community, whereas increasing values represent progressively greater microbiota deviation. For visualization of longitudinal microbiota dynamics, dysbiosis scores were summarized at basal, pre-colitis, and post-colitis time points. The reference-based interpretation of microbiota deviation was adapted from previously described approaches [32].

2.11. Fecal–Cecal Microbial Functional Continuity Analysis

Microbial functional continuity between the pre-colitis fecal microbiota and post-colitis cecal microbiota was evaluated using predicted microbial pathway abundance profiles. A common abundance threshold, defined as the 25th percentile of all positive pathway abundance values across the dataset, was applied to all experimental groups. A pathway was considered prevalent within a sampling compartment when its abundance exceeded this threshold in at least 50% of samples. Pathways were subsequently classified as shared (prevalent in both fecal and cecal samples), fecal only, cecum only, or neither (pathways that did not meet the prevalence criterion in either compartment). Pathways classified as neither were excluded from the displayed proportions.

2.12. Microbial Correlation-Network and Temporal Rewiring Analysis

Genus-level microbial association networks were constructed independently for each experimental group using 1-week fecal and post-DSS cecal relative abundances profiles. Genera with insufficient observations or invariant abundance profiles were excluded before correlation analysis.

Temporal network remodeling was characterized by classifying associations as gained (detected only in the cecal network), lost (detected only in the fecal network), retained (present at both sampling stages with the same direction of association), or sign-switched (present at both stages but changing from a positive to negative correlation or vice versa). The numbers of edges in each category were used to characterize treatment-associated microbial network rewiring. Post-DSS network topology was further assessed using node degree, defined as the number of robust correlations connected to an individual genus, and the 15 genera with the highest degree were designated as the major network hubs for visualization. Higher node degree therefore represents greater connectivity of a genus within the corresponding microbial association network.

2.13. Statistical Analysis

All statistical analyses and data visualization were performed using R version 4.6.1 (R Foundation for Statistical Computing, Vienna, Austria), except for analyses conducted using QIIME 2 and MicrobiomeAnalyst. For parametric analyses, model assumptions were evaluated through residual diagnostics, including the Shapiro–Wilk test for normality, normal Q–Q plots, and residual-versus-fitted plots to examine variance patterns [33]. Deviations from normality and homogeneity of variance were identified and considered when interpreting the statistical results. Unless otherwise specified, statistical significance was defined as $p < 0.05$, and Benjamini–Hochberg correction was used where multiple-testing-adjusted results were evaluated. For longitudinal clinical outcomes, linear mixed-effects models were used to account for repeated measurements within individual mice. Within-group comparisons between baseline and one week of dietary supplementation were performed using paired t-tests (Figure 2). Differences among experimental groups for the outcomes presented in Figures 3 and 4 were assessed using one-way analysis of variance (ANOVA), followed by Tukey's honestly significant difference (HSD) post hoc test for multiple pairwise comparisons. Microbial α-diversity was evaluated using Shannon entropy, observed features, Faith's phylogenetic diversity, and Pielou's evenness, whereas differences in β-diversity were assessed using permutational multivariate analysis of variance (PERMANOVA) based on UniFrac distance matrices. Nonparametric tests were applied to relevant microbial abundance comparisons. Differentially abundant bacterial genera were identified using linear discriminant analysis effect size (LEfSe) implemented in MicrobiomeAnalyst. For fecal–cecal microbial functional continuity analysis, the numbers of shared and non-shared pathways (fecal-only plus cecum-only) were compared between each experimental group and the DSS group using two-sided Fisher's exact tests. The resulting p-values were adjusted for multiple comparisons using the Benjamini–Hochberg procedure, with an FDR-adjusted p-value (q-value) < 0.05 considered statistically significant. For microbial correlation-network analysis, pairwise genus-level associations were evaluated using Spearman's rank correlation coefficients. Robust associations were defined as those with an absolute correlation coefficient $|\rho| \geq 0.70$ and $p < 0.05$. Benjamini–Hochberg FDR-adjusted p-values were additionally calculated to evaluate the robustness of associations to multiple testing. For cumulative water-consumption analysis, daily water consumption was summarized separately during dietary supplementation (Days 1–7) and DSS administration (Days 8–14). Each cage, containing two mice, was considered an independent experimental

unit ($n = 4$ cages per group). Differences among experimental groups were evaluated separately for each period using one-way ANOVA followed by Tukey's HSD post hoc test.

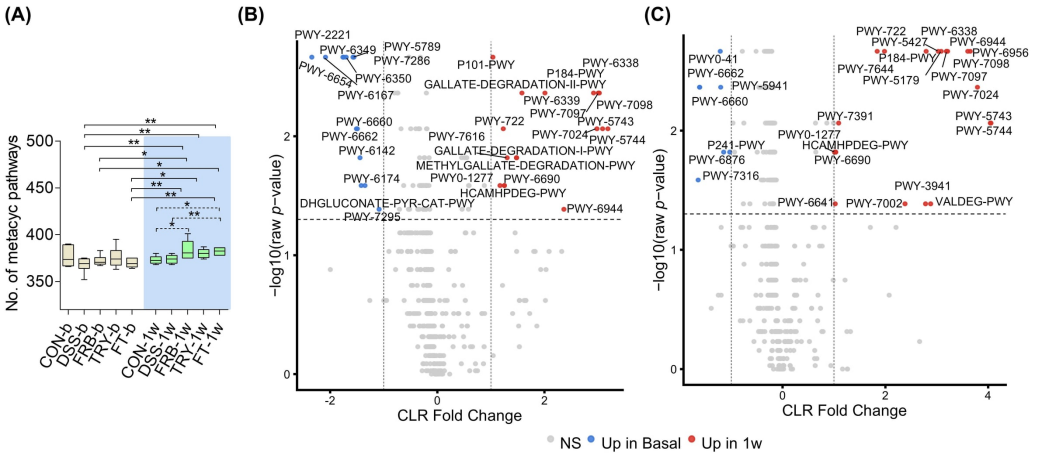


Figure 2. Effects of dietary interventions on predicted gut microbial metabolic pathways before DSS-induced colitis. (**A**) Number of predicted MetaCyc pathways across experimental groups at baseline (-b) and after one week (-1w) of dietary intervention before DSS exposure. Box plots represent the distribution of pathway richness within each group, with statistical significance indicated by brackets and asterisks. Within-group comparisons between baseline and one week were performed using paired *t*-tests. (**B**,**C**) Volcano plots showing differential MetaCyc pathway abundance between baseline and 1-week fecal microbiota in the FRB (**B**) and FT (**C**) groups, respectively. The x-axis represents centered log-ratio (CLR) fold change, and the y-axis represents −log10 (*p*-value). Positive CLR fold changes indicate pathways enriched after one week of dietary intervention, whereas negative values indicate pathways enriched at baseline. Dashed vertical and horizontal lines indicate the predefined fold-change and statistical significance thresholds, respectively. Significantly altered pathways are labeled by their MetaCyc pathway identifiers. Grey points indicate non-significant pathways. CLR, centered log-ratio; * $p < 0.05$ and ** $p < 0.01$. $n = 6$ per group.

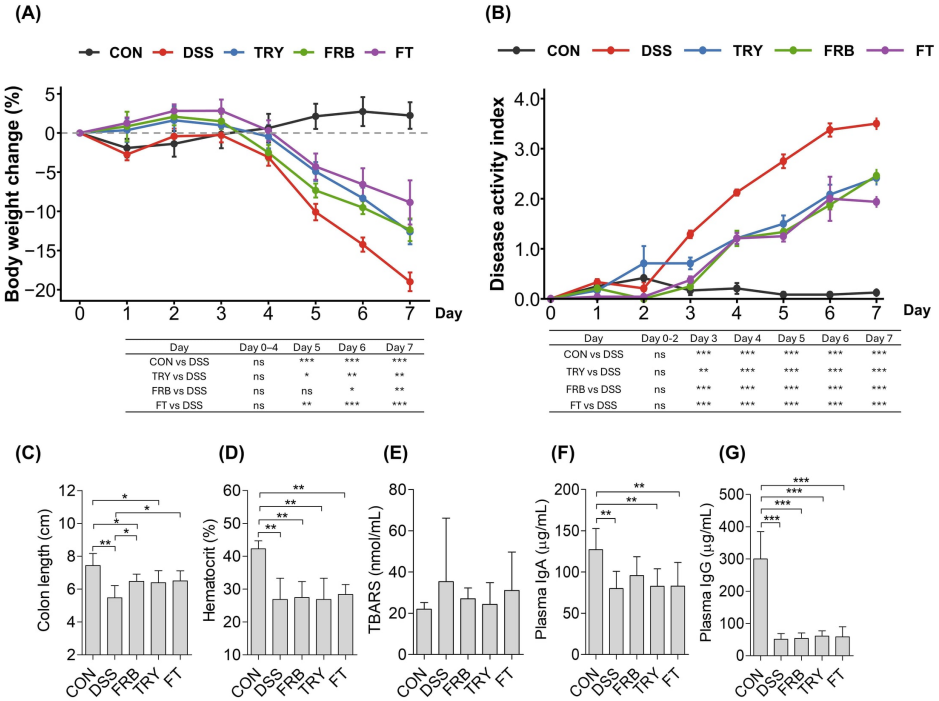


Figure 3. *Cont.*

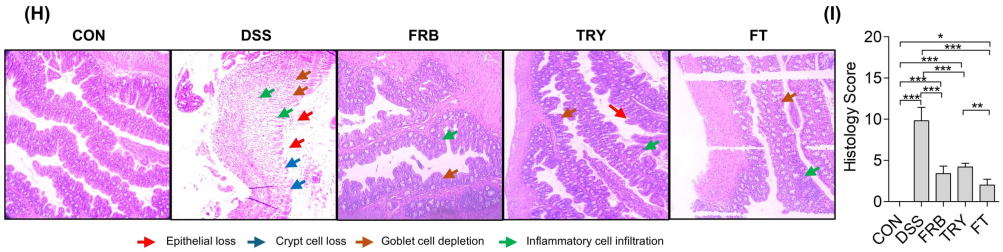


Figure 3. FRB and TRY ameliorate clinical severity in DSS-induced colitis. (**A**) Body weight changes relative to baseline (day 0) and (**B**) disease activity index (DAI) during the experimental period. Data are presented as the mean ± SEM (n = 8 mice/group). Statistical differences among groups at each time point were analyzed using linear mixed-effects models with group, day, and their interaction as fixed effects and mouse as a random effect, followed by Tukey-adjusted pairwise comparisons. Different lowercase letters indicate significant differences among groups within the same day ($p < 0.05$); groups sharing at least one letter are not significantly different. (**C**) Colon length as an indicator of DSS-induced colonic inflammation. (**D**) Hematocrit levels. (**E**) Thiobarbituric acid-reactive substances (TBARS) as an indicator of lipid peroxidation and oxidative stress. (**F**) Plasma immunoglobulin A (IgA) levels. (**G**) Plasma immunoglobulin G (IgG) levels. For panels (**A**–**G**), n = 8 mice/group. (**H**) Representative hematoxylin and eosin (H&E)-stained colon sections from the CON, DSS, FRB, TRY, and FT groups. (**I**) Quantitative histopathological assessment of colonic injury based on the indicated histological parameters. Five mice per group were analyzed using two histological slides per mouse (n = 5 mice/group). Statistical differences among groups were assessed using one-way analysis of variance (ANOVA), followed by Tukey's honestly significant difference (HSD) post hoc test for multiple pairwise comparisons. Statistical significance is indicated as * $p < 0.05$, ** $p < 0.01$, and *** $p < 0.001$.

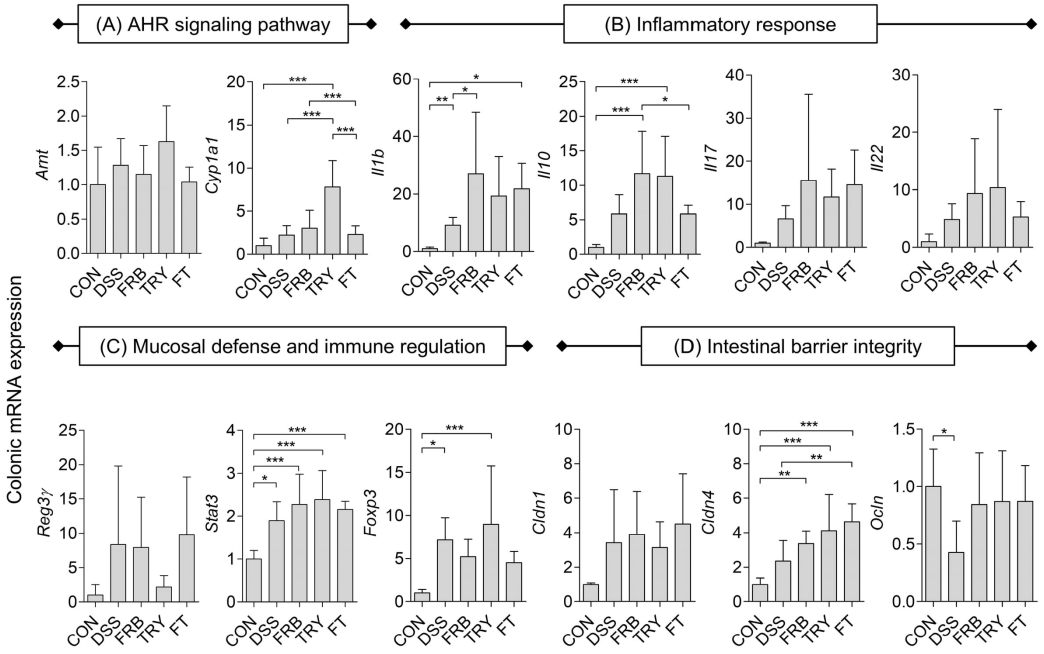


Figure 4. Colonic transcript expression of genes involved in (**A**) aryl hydrocarbon receptor (AHR) signaling pathway (*Arnt* and *Cyp1a1*), (**B**) inflammatory response (*Il1b*, *Il10*, *Il17* and *Il22*), (**C**) mucosal defense and immune response (*Reg3g*, *Stat3*, and *Foxp3*), and (**D**) intestinal barrier integrity (*Cldn1*, *Cldn4*, and *Ocln*) in colonic tissue. mRNA expression was determined by reverse transcription quantitative polymerase chain reaction and expressed relative to the appropriate reference gene (*Efe1a1*). Data are presented as mean ± SD. Statistical differences among groups were assessed using one-way analysis of variance (ANOVA), followed by Tukey's honestly significant difference (HSD)

post hoc test for multiple pairwise comparisons. Statistical significance between groups is indicated by brackets: * $p < 0.05$, ** $p < 0.01$, and *** $p < 0.001$. $n = 6$–8 per group.

3. Results

3.1. Experimental Design and Gut Microbiota Changes Before DSS Treatment

To investigate whether dietary FRB and tryptamine supplementation influence gut microbial dynamics and the subsequent response to intestinal inflammatory challenge, a longitudinal dietary intervention study was conducted. As differences in drinking-water intake may influence DSS exposure and subsequent colitis severity, water consumption was also assessed throughout the experimental period. Cumulative water consumption was evaluated separately during pre-colitis and colitis period (Supplementary Figure S1). No significant differences were observed among experimental groups during pre-colitis period. During colitis, DSS administration, cumulative water consumption did not differ significantly among DSS-exposed groups (DSS, FRB, TRY, and FT), although the FT group exhibited significantly higher consumption than CON ($p = 0.0014$).

Fecal microbial communities were analyzed at baseline and after one week of dietary supplementation, prior to DSS exposure. Baseline microbial communities were highly similar across all groups, with *Akkermansia* (CON: 24.43 ± 3.42%; DSS: 25.30 ± 2.85%; FRB: 24.83 ± 1.79%; TRY: 22.42 ± 3.90%; FT: 20.63 ± 2.46%), and *JAGBWK01*, (17.32 ± 1.78%, 12.77 ± 4.05%, 11.44 ± 2.90%, 13.91 ± 3.71%, and 13.51 ± 1.57%, respectively) representing the dominant genera (Figure 1B). After one week of dietary intervention, several genera differed significantly among groups. *Alloprevotella* was enriched in FRB (12.08 ± 2.68%) and FT (10.43 ± 3.43%) compared with DSS (1.49 ± 0.82%) and TRY (1.18 ± 0.88%). FT also showed the highest abundances of *Alistipes_A_871400* (5.49 ± 1.04%), *Duncaniella* (1.62 ± 0.25%), *Phocaeicola_A* (7.42 ± 1.18%), and *Prevotella* (2.04 ± 0.18%), with significant group differences indicated by non-overlapping statistical letters ($p < 0.05$). The FT group exhibited the greatest compositional shift, characterized by reduced *Akkermansia* together with enrichment of *Alistipes_A_871400*, *Muribaculum*, and other *Bacteroidota*-associated genera, indicating a distinct microbial response to the combined treatment (Supplementary Figure S2). Along with the genus level, the overall relative abundance based on family level is shown in Supplementary Figure S3.

Alpha diversity showed no significant differences among groups at baseline (Figure 1C). After one week, Shannon entropy and observed features remained largely unchanged, whereas Faith's PD and Pielou's evenness showed modest reductions in several treatment groups, indicating effects of short-term dietary supplementation on overall microbial diversity (Figure 1C). Beta diversity, which quantifies the compositional dissimilarity between microbial communities, was assessed using unweighted UniFrac distances, a phylogenetic metric based on the presence or absence of taxa weighted by evolutionary relatedness. This analysis revealed significant temporal shifts in gut microbial composition in the FRB ($p = 0.004$) and FT ($p = 0.004$) groups following one week of dietary intervention, whereas no significant shifts were observed in the CON ($p = 0.190$), DSS ($p = 0.124$), or TRY ($p = 0.082$) groups (Figure 1D). These findings indicate that FRB-containing diets rapidly and directionally reshaped gut microbial community structure prior to DSS challenge.

LEfSe analysis identified microbial taxa associated with dietary intervention (Figure 1E,F). In the FRB group, baseline samples were enriched with *Akkermansia*, *Dysosmobacter*, *Parasutterella*, *Streptococcaceae*, and *Anaerotignaceae*, whereas one-week samples were enriched with *Duncaniella*, *Prevotella*, *Alistipes_A_871400*, and *Phocaeicola_A*. In the FT group, baseline enrichment included *Akkermansia*, *Eubacterium_R*, *JAGBWK01*, *Parasutterella*, and *Anaerotruncus*, while one-week supplementation enriched *Nanosyncoccus*,

UMGS1994, *UBA3263*, *Duncaniella*, *Prevotella*, and *Alistipes_A_871400*. Shared enrichment of *Duncaniella*, *Prevotella*, and *Alistipes_A_871400* suggests a common microbial response to FRB supplementation, whereas FT induced additional taxonomic diversification.

3.2. Functional Remodeling of the Microbiome During Dietary Intervention

To investigate whether the observed taxonomic changes were accompanied by functional alterations, PICRUSt2 was used to predict MetaCyc metabolic pathways from the 16S rRNA gene amplicon sequencing data (Figure 2). The total number of predicted MetaCyc pathways increased significantly after one week of FRB and FT supplementation compared with baseline ($p = 0.0157$; $p = 0.0028$ respectively), whereas minor change was observed in the CON, DSS, and TRY groups (Figure 2A). Differential pathway analysis further demonstrated functional remodeling following dietary intervention. In the FRB group, pathways involved in carbohydrate utilization and aromatic compound metabolism were significantly altered after one week, including Gallate degradation, Methylgallate degradation, DHGLUCONATE-PYR-CAT, and several biosynthetic pathways (Figure 2B). The FT group exhibited broader functional alterations, with enrichment of multiple biosynthetic and degradation pathways, including PWY-7024, PWY-7097, PWY-7098, PWY-6944, and PWY-5743, indicating greater metabolic restructuring than FRB alone (Figure 2C).

3.3. Effects of Fermented Rice Bran and Tryptamine Supplementation on Clinical, Histological, Oxidative Stress, and Immunological Outcomes in DSS-Induced Colitis

To determine whether pre-colitis microbiome modulation translated into protection against intestinal inflammation, we next evaluated clinical, oxidative stress, immunological, and histological outcomes following DSS-induced colitis (Figure 3). Following DSS administration, the DSS group exhibited a progressive decline in body weight, accompanied by a marked increase in disease activity index (DAI), confirming the development of DSS-induced colitis (Figure 3A,B). After DSS administration, body weight remained relatively stable during the early phase; however, a pronounced reduction was observed in DSS-treated mice from Day 5 onward ($p < 0.05$). At Day 7, the DSS group showed the highest body weight loss reaching approximately 18%, whereas FRB, TRY, and FT significantly avoided weight loss, with FT showing the least reduction among the DSS-treated groups (Figure 3A). FRB, TRY, and FT did not differ significantly ($p > 0.05$) from one another on Day 7.

Consistent with the changes in body weight, DAI scores increased progressively following DSS exposure. DAI similarly increased progressively in the DSS group and was significantly higher than the intervention groups during the later phase of DSS exposure (Figure 3B; $p < 0.05$), showed the most pronounced increase, whereas supplementation with TRY and FRB reduced the severity of clinical symptoms relative to DSS, although their DAI scores remained elevated (Figure 3B; $p > 0.05$). Collectively, these findings indicate that FRB, TRY, and their combination mitigated the DSS-induced clinical manifestations.

Colonic length was significantly reduced in the DSS group compared with CON ($p = 0.0000106$), while FRB and FT significantly attenuated the DSS-induced colon shortening ($p = 0.036544$ and 0.039184, respectively; Figure 3C). There were no significant differences among FRB, TRY, FT, which may indicate that dietary supplementation confers a protective effect against DSS-induced colon shortening. Hematocrit was significantly reduced by DSS compared with CON ($p = 5.85 \times 10^{-6}$) and remained significantly lower in FRB ($p = 6.28 \times 10^{-6}$), TRY ($p = 5.85 \times 10^{-6}$), and FT ($p = 1.95 \times 10^{-5}$) compared with CON (Figure 3D). In contrast, plasma TBARS levels, assessed as an indirect indicator of lipid peroxidation, did not differ significantly among groups (Figure 3E). Plasma IgA concentrations were significantly lower in the DSS, TRY, and FT groups than in CON

($p = 0.003324$, 0.006412, and 0.006617, respectively), while FRB did not differ significantly from CON (Figure 3F). Plasma IgG was markedly reduced in all DSS-exposed groups compared with CON ($p \leq 3.51 \times 10^{-12}$), with no significant differences among DSS, FRB, TRY, and FT (Figure 3G). Although circulating IgA is immunologically linked to mucosal immune responses, plasma IgA concentrations do not directly reflect intestinal secretory IgA levels or function; therefore, the observed changes in plasma IgA should be interpreted as systemic humoral immune responses rather than direct evidence of altered intestinal mucosal immunity [34].

Histological examination further confirmed DSS-induced colonic injury (Figure 3H). Colonic tissues from the CON group showed largely preserved mucosal architecture with intact epithelial and crypt structures. In contrast, all of the DSS-treated mice exhibited a different range of histopathological damage, like epithelial disruption, loss of normal crypt architecture, and inflammatory cell infiltration. Consistent with microscopic observations, the histology score (Figure 3I) was markedly increased in the DSS group compared with the CON group ($p = 2.51 \times 10^{-12}$). Compared with DSS, histological scores were significantly reduced in FRB ($p = 5.48 \times 10^{-9}$), TRY ($p = 5.26 \times 10^{-8}$), and FT ($p = 1.65 \times 10^{-10}$). Although FT exhibited the lowest histological score among the intervention groups, a significant difference was observed only between FT and TRY ($p = 0.008901$), whereas FT and FRB did not differ significantly.

Although varying degrees of epithelial injury remained evident among the intervention groups, these findings indicate that FRB, TRY, and combined FRB–TRY supplementation differentially attenuated DSS-associated histopathological damage.

3.4. mRNA Extraction and Analysis with Reverse Transcription Quantitative Polymerase Chain Reaction (RT-qPCR) of Colon Tissues

To investigate the molecular responses associated with the dietary interventions, we assessed colonic transcript levels of genes spanning AHR-related signaling, mucosal cytokines, immune regulation, and epithelial barrier function (Figure 4). For AHR-associated genes, *Arnt* did not differ among groups, whereas *Cyp1a1* was markedly induced in TRY relative to CON ($p = 7.53 \times 10^{-7}$), DSS ($p = 0.0000251$), FRB ($p = 0.000178$), and FT ($p = 0.0000175$). Notably, the pronounced *Cyp1a1* induction observed in the TRY group was not maintained in the FT group, indicating that the combined FRB and TRY supplementation was associated with a distinct *Cyp1a1* expression pattern rather than simply reproducing the response observed with TRY alone (Figure 4A).

The pro-inflammatory gene *Il1b* was significantly elevated in FRB (adjusted $p = 0.0021$) and FT ($p = 0.0197$) compared with CON, whereas TRY showed a nonsignificant increase. Compared with DSS, *Il1b* expression was significantly higher only in FRB ($p = 0.0459$), while DSS itself did not differ significantly from CON ($p = 0.7017$). The anti-inflammatory gene *Il10* was increased in FRB ($p = 0.000119$) and TRY ($p = 0.000210$) compared with CON. Furthermore, FT exhibited significantly lower *Il10* expression than FRB ($p = 0.04898$). No significant differences were observed for *Il17* or *Il22* (Figure 4B).

Among mucosal defense and regulatory genes, *Reg3g* was unchanged, whereas *Stat3* was elevated in DSS and all intervention groups. *Foxp3* was increased in DSS and showed the greatest induction in TRY but not in FRB and FT (Figure 4C).

Among barrier-related genes, *Cldn1* showed no significant differences, whereas *Cldn4* was increased in DSS, FRB, TRY, and FT relative to CON, consistent with a compensatory epithelial repair response common to injury and all interventions. *Ocln* was significantly reduced by DSS and showed a non-significant tendency toward recovery with FRB, TRY, and FT (Figure 4D).

Overall, TRY strongly induced *Arnt/Cyp1a1* and *Foxp3*, while FRB increased *Il1b* and *Il10* and modulated TRY-induced *Cyp1a1* expression, suggesting that FRB provides a regulatory matrix and TRY acts as a functional effector metabolite.

3.5. Cecal Microbiota After DSS-Induced Colitis

To determine whether the protective effects of dietary supplementation were associated with sustained alterations in the gut microbiota after DSS-induced colitis, cecal microbial community, and its predicted metabolic functions were evaluated. Alpha diversity differed significantly among treatment groups (Figure 5A). Compared with DSS, FRB showed higher Shannon entropy, observed features, and Pielou's evenness ($p < 0.01$). Principal coordinate analysis (PCoA) revealed distinct clustering among dietary groups with pairwise PERMANOVA identifying multiple significant differences among groups (Figure 5B; q < 0.05). In particular, CON differed significantly from DSS, TRY, and FT, while DSS also differed from FRB and FT, indicating treatment-dependent restructuring of the cecal microbial community following DSS challenge (Figure 5C). LEfSe analysis further demonstrated treatment-specific bacterial signatures (Figure 5D). The DSS group was enriched in *Peptostreptococcaceae*, *Clostridium_T*, and *Granulimonas*, whereas the FRB group showed enrichment of *Oscillospiraceae*, *Nanosyncoccus*, *Paludihabitans*, and *Evtepia*. The FT group was characterized by increased *Muribaculaceae*, *Angelakisella*, *CAG_314*, *Oscillospiraceae*, and *Nanosyncoccus*, indicating that FRB-containing diets established distinct microbial communities following DSS-induced colitis. Functional prediction also revealed clear pathway differences among treatment groups, with FRB and FT displaying metabolic profiles distinct from both CON and DSS groups, pathways including glycolysis (GLYCOLYSIS), galactose degradation (GALACTARDEG-PWY), L-lysine biosynthesis (PWY-2941), L-isoleucine biosynthesis (ILEUSYN-PWY), and glycogen degradation (GLYCOCAT-PWY) (Figure 5E).

3.6. FRB Attenuates DSS-Induced Microbiota Dysbiosis and Preserves Functional and Ecological Organization

To determine whether dietary interventions influenced microbiota stability during the development of colitis, we first quantified longitudinal community deviation from the healthy basal microbiota using Bray–Curtis dissimilarity (Figure 6A). Microbial communities remained relatively close to the healthy reference at baseline and after the 1-week dietary intervention. Following DSS exposure, however, the DSS group exhibited a pronounced increase in dysbiosis, indicating substantial disruption of the microbial community. FRB and TRY supplementation attenuated this DSS-associated divergence to different extents, with the FRB-containing interventions showing greater preservation of community structure. These findings indicate that dietary preconditioning, particularly with FRB, was associated with increased compositional resilience of the gut microbiota during DSS-induced intestinal inflammation. DSS exposure markedly increased microbiota dysbiosis, whereas this increase was significantly attenuated by FRB and FT (both adjusted $p < 0.001$; Figure 6A). In contrast, TRY did not significantly differ from DSS ($p = 0.236$).

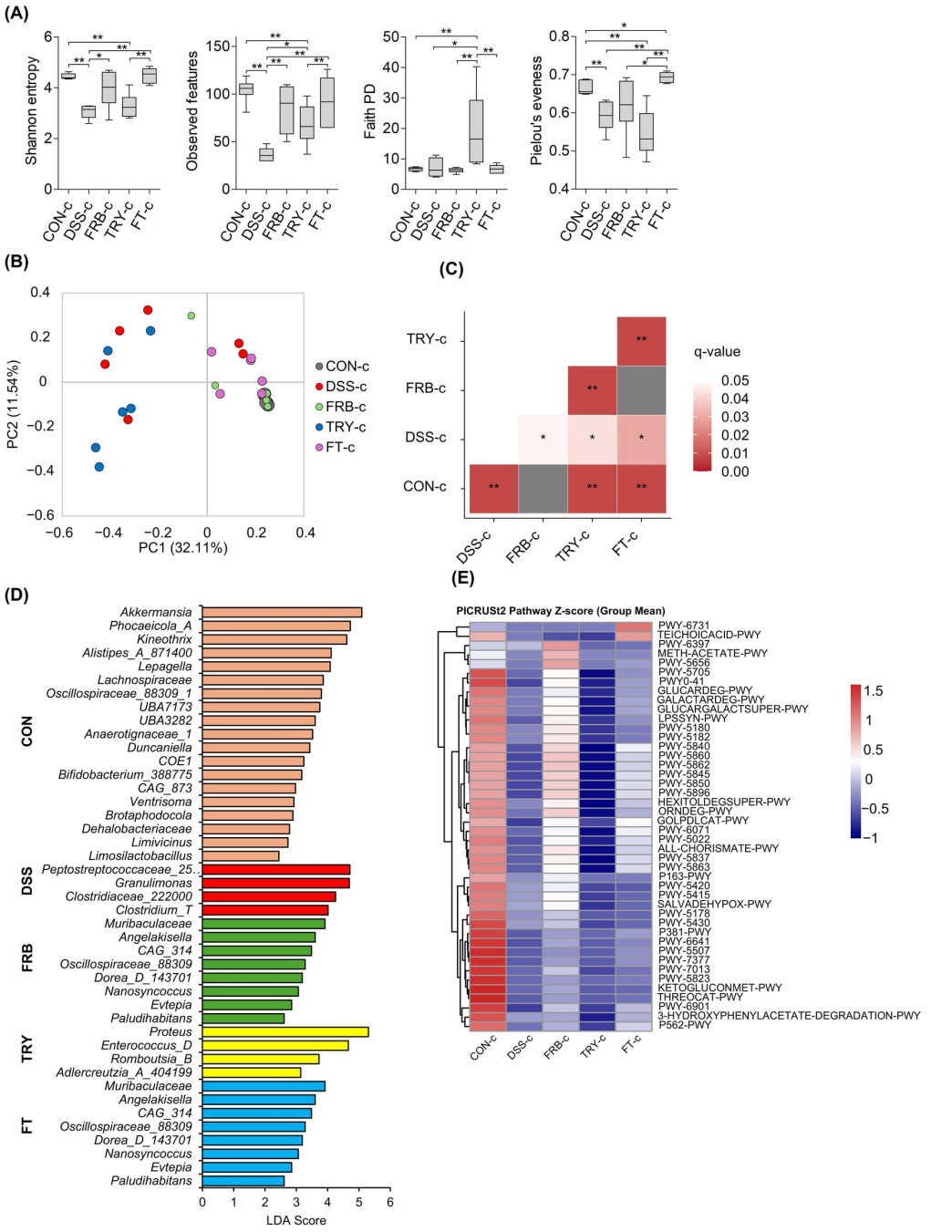


Figure 5. Effects of dietary fermented rice bran and tryptamine supplementation on the cecal microbiota and predicted microbial functions following DSS-induced colitis. (**A**) Alpha diversity of the cecal microbiota assessed using Shannon entropy, observed features, Faith's phylogenetic diversity (Faith PD), and Pielou's evenness. (**B**) Principal coordinate analysis (PCoA) of cecal microbial communities based on unweighted UniFrac distances. Each point represents an individual mouse, and the percentages on the axes indicate the proportion of variation explained by the corresponding principal coordinates. (**C**) Pairwise PERMANOVA analysis of cecal microbial community composition among treatment groups. Heatmap colors represent FDR-adjusted q-values, with asterisks indicating significant pairwise differences. (**D**) Linear discriminant analysis effect size (LEfSe) analysis showing bacterial taxa differentially enriched among the experimental groups. Horizontal bars represent linear discriminant analysis (LDA) scores, and colors indicate the treatment groups in which the corresponding taxa were enriched. (**E**) Heatmap of predicted MetaCyc pathway abundances generated using PICRUSt2. Values are presented as row-scaled Z-scores to illustrate relative differences in predicted pathway abundance among groups. Hierarchical clustering was applied to pathways based

on their abundance profiles. Statistical significance is indicated as * $p < 0.05$ and ** $p < 0.01$. PCoA, principal coordinate analysis; PERMANOVA, permutational multivariate analysis of variance; FDR, false discovery rate; LEfSe, linear discriminant analysis effect size; LDA, linear discriminant analysis; PICRUSt2, Phylogenetic *Investigation* of Communities by Reconstruction of Unobserved States 2.

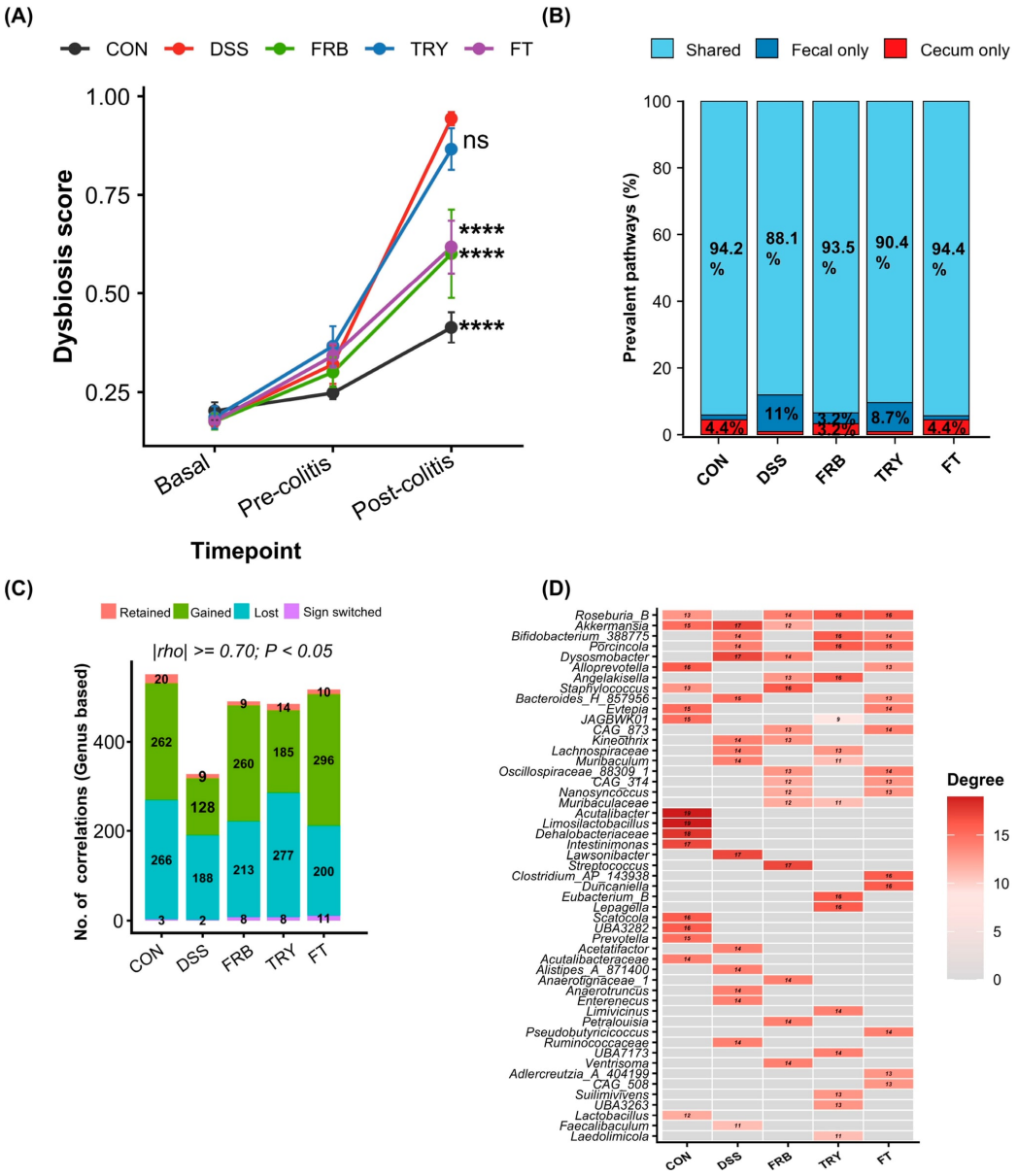


Figure 6. Fermented rice bran and tryptamine modulate gut microbial community dynamics, predicted functional continuity, and network organization during DSS-induced colitis. (**A**) Longitudinal changes in gut microbial dysbiosis in mice. Dysbiosis was quantified as the Bray–Curtis dissimilarity of each sample from the healthy reference community and is presented as mean ± SEM. **** $p < 0.001$. (**B**) Continuity of predicted microbial functions between pre-DSS fecal (1 week) and post-DSS cecal microbiota. PICRUSt2-predicted MetaCyc pathways were classified as shared between the two sampling points, fecal-specific, or cecum-specific; percentages within stacked bars indicate the proportion of pathways in each category. (**C**) Temporal rewiring of genus-level microbial association networks between pre-DSS fecal (1 week) and post-DSS cecal microbiota. Strong associations were defined as Spearman's $|\rho| \geq 0.70$ and $p < 0.05$ and classified as retained, gained, lost, or sign-switched according to changes in correlation status between sampling points. Numbers within bars indicate the number of associations in each category. (**D**) Heatmap showing highly connected genera in post-DSS cecal microbial networks across experimental groups. Network connectivity was quantified by node

degree, representing the number of strong microbial associations involving each genus; higher values indicate greater connectivity. Grey cells indicate genera that were not identified among the selected top hubs in the corresponding group. $n = 6$ per group. Statistical significance was set at FDR-adjusted $p < 0.05$. $n = 6$ per group. CON, control; DSS, dextran sulfate sodium; FRB, fermented rice bran; TRY, tryptamine; FT, fermented rice bran plus tryptamine; PCoA, principal coordinate analysis; PICRUSt2, Phylogenetic Investigation of Communities by Reconstruction of Unobserved States 2.

We next investigated whether this compositional resilience was accompanied by preservation of predicted microbial functions by comparing MetaCyc pathway prevalence between the 1-week fecal and post-DSS cecal microbiota (Figure 6B). Pathways were classified as shared, fecal-only, or cecum-only according to their prevalence in the two compartments. The CON group exhibited 94.2% shared pathways, whereas DSS reduced this proportion to 88.1%, consistent with increased loss or restructuring of the pre-existing predicted functional repertoire. In contrast, FRB maintained 93.5% pathway continuity, approaching the level observed in CON. TRY showed intermediate preservation (90.4%), whereas the combined FT treatment exhibited the highest continuity (94.4%).

Relative to DSS, the distribution of pathway conservation differed significantly in CON (OR = 0.459, FDR = 0.012), FRB (OR = 0.513, FDR = 0.021), and FT (OR = 0.439, FDR = 0.012), whereas TRY did not differ significantly from DSS (OR = 0.780, FDR = 0.379), were based on Fisher's exact tests followed by Benjamini–Hochberg correction.

Because preservation of individual pathways does not capture changes in microbial ecological organization, we next examined temporal rewiring of genus-level microbial association networks between the 1-week fecal and post-DSS cecal stages (Figure 6C). DSS displayed a comparatively restricted network response, with 128 gained, 188 lost, 9 retained, and 2 sign-switched correlations. In contrast, FRB showed substantially greater network reorganization, comprising 260 gained, 213 lost, 9 retained, and 8 sign-switched correlations. TRY exhibited 185 gained, 277 lost, 14 retained, and 8 sign-switched correlations, whereas FT displayed the greatest number of newly established associations, with 296 gained, 200 lost, 10 retained, and 11 sign-switched correlations. CON showed 262 gained, 266 lost, 20 retained, and 3 sign-switched correlations.

Thus, DSS was characterized by relatively limited formation of new robust microbial associations compared with CON and the FRB-containing interventions. In particular, FRB and FT generated approximately twofold more gained correlations than DSS (260 and 296 versus 128, respectively), indicating extensive treatment-associated restructuring of microbial associations during the transition from the pre-colitis fecal state to the post-colitis cecal environment. TRY differed from the FRB-containing treatments by showing a greater predominance of lost than gained associations (277 versus 185), suggesting a distinct pattern of ecological restructuring.

We subsequently examined whether these differences in network rewiring were accompanied by treatment-specific organization of highly connected genera in the post-DSS cecal microbiota (Figure 6D). The CON network was dominated by *Acutalibacter* and *Limosilactobacillus*, followed by *Dehalobacteriaceae* and *Intestinimonas*. DSS markedly altered this hub architecture, with *Akkermansia*, *Dysosmobacter*, and *Lawsonibacter* emerging as the most highly connected genera.

Distinct hub configurations were observed following each dietary intervention. The FRB network was characterized by *Streptococcus* and *Staphylococcus*, together with multiple moderately connected genera. In TRY, *Lepagella*, *Bifidobacterium_388775*, *Angelakisella*, *Eubacterium_B*, *Porcincola*, and *Roseburia_B* each reached a degree of 16. The combined FT intervention generated another distinct network configuration, with *Duncaniella*, *Clostridium_AP_143938*, and *Roseburia_B* among the most connected genera, followed by *Porcincola*.

Notably, *Roseburia_B* remained highly connected across several treatment networks, whereas many other high-degree genera were treatment-specific.

Collectively, these analyses reveal complementary aspects of microbiome resilience during DSS-induced colitis. DSS exposure was associated with increased compositional dysbiosis, reduced persistence of predicted metabolic pathways, and altered microbial network organization. FRB-containing interventions were associated with reduced community deviation, greater predicted functional continuity, and extensive establishment of new microbial associations.

4. Discussion

The present study demonstrated that FRB-containing diets could precondition the gut microbiota prior to an inflammatory challenge, whereas TRY alone did not induce a comparable community-level shift. Following DSS challenge, FRB-containing interventions were associated with reduced microbial dysbiosis, higher similarity in PICRUSt2-predicted functional profiles between pre-DSS fecal and post-DSS cecal microbiota, and extensive ecological network reorganization. The effects of a fermented-food matrix may arise from interactions among fermentable substrates, microbial populations, metabolites, and host responses that cannot be reproduced by supplementation with a single metabolite [35].

In the present study, FRB was prepared from zinc-biofortified rice bran using a probiotic consortium. However, subsequent drying at 40–60 °C may have affected microbial viability, and post-drying viable microbial counts were not determined. Therefore, the relative contributions of surviving microorganisms, fermentation-derived metabolites, and other bioactive components of the FRB matrix to the observed protective effects remain unclear. Nevertheless, fermented products may exert beneficial effects independently of microbial viability [36].

These findings highlight the potential importance of dietary modulation before inflammatory challenge. Rather than acting only after inflammation is established, fermented food interventions may influence the ecological state of the gut microbiota before perturbation. This concept is consistent with microbiome resilience, whereby the initial ecological state can influence community responses to disturbance [37]. Supporting its translational relevance, a fermented-food-rich diet increased microbiota diversity and reduced inflammatory markers in healthy adults [38]. Thus, dietary preconditioning warrants further investigation as a potential strategy for promoting intestinal resilience. Although Faith's phylogenetic diversity and Pielou's evenness decreased following dietary intervention, these changes require careful interpretation. Reduced phylogenetic diversity and evenness may indicate a narrower and less balanced microbial community, potentially affecting ecological resilience. However, lower alpha diversity does not necessarily imply adverse microbial function [39,40] as dietary interventions may selectively enrich particular taxa. In the present study, FRB-containing diets were associated with reduced post-DSS dysbiosis and greater predicted functional continuity, suggesting selective microbial restructuring rather than uniformly detrimental changes. Nevertheless, the potential negative consequences of reduced diversity cannot be excluded without further functional validation.

Previous studies have shown that FRB attenuates DSS-induced intestinal injury through modulation of inflammation, barrier function, microbial composition, and microbial metabolites [5,6,10]. Our findings extend these observations by showing that significant microbial restructuring occurs before DSS exposure if diet is supplemented earlier, supporting a microbiota-preconditioning effect that cannot be explained solely as a consequence of reduced inflammation. However, the systemic biomarkers measured in this study also require careful interpretation in relation to intestinal inflammation and oxidative stress. Although circulating IgA is immunologically linked to mucosal immune responses and

host–microbiota interactions, plasma IgA concentrations do not directly reflect intestinal secretory IgA levels or function [41]. Therefore, the observed plasma IgA changes should be interpreted as systemic humoral immune responses rather than direct evidence of altered intestinal mucosal immunity. Similarly, although oxidative stress contributes to intestinal inflammatory injury, the absence of significant differences in plasma TBARS suggests that the protective effects of FRB and TRY were not accompanied by detectable reductions in systemic lipid peroxidation. However, plasma TBARS may not adequately reflect localized intestinal oxidative damage, and further tissue-specific assessments are required to clarify the potential contribution of oxidative stress to intestinal protection.

Interestingly, TRY supplementation attenuated DSS-induced intestinal injury without inducing the pronounced pre-DSS microbial community restructuring observed with FRB-containing diets. This suggests that the protective effects of TRY may not require broad remodeling of the gut microbiota and may instead involve more direct host-associated mechanisms. The strong induction of *Cyp1a1* in the TRY group further supports the involvement of host signaling pathways [18,42], potentially including AHR-associated responses, although direct activation of AHR by TRY cannot be concluded from the present data. AHR signaling can promote IL-22 production, particularly through intestinal ILC3s and T cells, thereby contributing to epithelial barrier maintenance and mucosal defense [43]. However, the absence of a significant increase in *Il22* expression in the TRY group suggests that the strong *Cyp1a1* response observed here was not accompanied by detectable activation of the downstream IL-22 response under the present experimental conditions. Alternatively, microbiota-derived TRY has been shown to activate epithelial serotonin receptor 4 (5-HT4R), promoting intestinal fluid secretion and gastrointestinal transit, while also enhancing colonic mucus release and attenuating experimental colitis [18,42]. These findings suggest that serotonin receptor-mediated effects on epithelial secretion, mucus-barrier function, and intestinal motility may represent alternative mechanisms of TRY-associated protection, although these pathways were not directly evaluated in the present study.

However, in the case of the predicted microbial metabolic functions, two carbohydrate-related pathways were particularly noteworthy: GALACTARDEG-PWY (galactarate degradation) and GLUCOSE1PMETAB-PWY (glucose-1-phosphate metabolism). These pathways contribute to microbial carbohydrate utilization and central carbon metabolism, respectively. Given that FRB contains dietary fibers and complex carbohydrates, their relatively higher predicted abundances in the FRB group may reflect a microbial metabolic response to the fermented dietary matrix. This observation highlights the potential role of FRB in shaping microbial carbohydrate-processing capacity during intestinal inflammation [44].

Overall, the microbial network analysis further revealed diet-specific ecological organizations. During the transition from the pre-colitis fecal microbiota to the post-colitis cecal microbiota, DSS showed relatively few gained correlations (128), whereas FRB and FT exhibited substantially greater network reorganization, with 260 and 296 gained correlations, respectively. TRY differed from the FRB-containing interventions, showing more lost than gained associations (277 vs. 185). The relatively small number of retained correlations across all groups indicates substantial network restructuring rather than simple preservation of the pre-colitis microbial network. However, these changes should be interpreted as a fecal-to-cecal network transition, because fecal and cecal microbial communities can differ in both taxonomic composition and functional activity [45]. Interesting, this interpretation is consistent that substantial reorganization of microbial co-occurrence network topology in inflammatory bowel disease, highlighting that intestinal inflammation can alter not only microbial composition but also community organization [46]. Notably, *Akkermansia* showed high connectivity in CON, DSS, and FRB, suggesting that its ecological importance along with high percentages of relative abundances were maintained while its

microbial associations were reorganized by diet. This is relevant because *A. muciniphila* has been associated with mucus-barrier integrity and modulation of intestinal inflammation, and experimental studies have demonstrated protective effects of specific *A. muciniphila* strains in DSS-induced colitis [47]. In contrast, other hubs were more treatment-specific, including *Streptococcus* in FRB and *Duncaniella*, *Clostridium_AP_143938*, and *Roseburia_B* in FT. Notably, the high connectivity of *Roseburia_B* in FT is potentially relevant because members of *Roseburia* are recognized butyrate producers, and reduced *Roseburia*-associated butyrate-production capacity has been reported in ulcerative colitis. Furthermore, *Roseburia intestinalis* and its metabolite butyrate attenuated experimental colitis and inflammatory responses reduced colon shortening, strengthened epithelial barrier integrity, and modulated the Treg/Th17 balance [48,49]. Thus, the high connectivity of *Roseburia_B* in FT may indicate its involvement in the reorganized cecal microbial network associated with intestinal protection. Previous studies suggest that fermented foods and dietary fibers can influence intestinal inflammation by modulating microbial populations and the production of bioactive metabolites, particularly short-chain fatty acids (SCFAs), which contribute to epithelial barrier integrity and mucosal immune regulation [50,51]. However, these effects may depend on the metabolic characteristics of individual bacterial species and strains rather than microbial diversity alone. Because 16S rRNA amplicon sequencing has limited strain-level resolution, further strain-resolved and metabolomic analyses are required to clarify these mechanisms [52].

Several limitations of this study should be acknowledged. First, only female mice were included, which may limit the generalizability of the findings to male animals, particularly given potential sex-dependent differences in intestinal immune responses and gut microbiota composition. Second, the relatively small sample size, particularly for microbiome analysis, may have limited the statistical power to detect subtle microbial differences. Third, predicted MetaCyc functions were inferred from 16S rRNA gene amplicon profiles using PICRUSt2 [31] and therefore represent functional potential rather than directly measured microbial genes or metabolites. Fourth, the absence of metabolomic analyses prevented direct assessment of microbial metabolites potentially involved in the protective effects of FRB and TRY. Fifth, microbial transplantation experiments were not performed; therefore, a causal relationship between the observed microbiota changes and improvements in colitis outcomes could not be established. Additionally, comparisons between pre-colitis fecal and post-colitis cecal microbiota involved different intestinal compartments and sampling time points, limiting conclusions regarding longitudinal microbial continuity. Future studies incorporating both sexes, larger sample sizes, shotgun metagenomics, metabolomics, and microbiota transplantation experiments are warranted to clarify the mechanisms underlying the protective effects of FRB and TRY against DSS-induced colitis. Overall, these findings highlight complementary nutritional strategies whereby FRB may act through microbiota preconditioning, while TRY may provide protection without requiring broad microbial restructuring. The FRB-TRY combination produced a distinct response rather than simply amplifying either intervention alone. This distinction is nutritionally relevant because it supports the development of fermented-food-based versus metabolite-targeted strategies according to the desired mode of intestinal modulation.

5. Conclusions

This study demonstrates that fermented rice bran (FRB), tryptamine (TRY), and their combination attenuated DSS-induced colitis, as evidenced by reduced weight loss, improved disease activity indices, and preservation of colon length. FRB-containing diets preconditioned the gut microbiota before inflammatory challenge and were associated with lower post-DSS dysbiosis, supporting greater ecological resilience. In contrast,

TRY attenuated intestinal injury despite persistent microbial dysbiosis, indicating potentially distinct host-associated protective responses and microbiome recovery. Changes in microbial diversity, community structure, and predicted carbohydrate-related metabolic pathways further supported the influence of dietary supplementation on gut microbial ecology. The combined FRB and TRY intervention also alleviated colitis, although the findings do not establish additive or synergistic effects. Collectively, these findings support our hypothesis that FRB and TRY may protect against intestinal inflammation through distinct but potentially complementary mechanisms. Further studies using shotgun metagenomics, metabolomics, and microbiota transplantation are needed to clarify the underlying causal mechanisms.

Supplementary Materials: The following supporting information can be downloaded at: https://www.mdpi.com/article/10.3390/foods15224137/s1, Figure S1: Cumulative water consumption during dietary supplementation and DSS administration. (A) Cumulative water consumption during the pre-colitis period (Days 1–7), before DSS exposure. (B) Cumulative water consumption during the colitis period (DSS administration period (Days 8–14). The experimental groups included control (CON), dextran sodium sulfate (DSS), fermented rice bran (FRB), tryptamine (TRY), and combined FRB and TRY supplementation (FT). During Days 8–14, all groups except CON received 3% DSS in drinking water. Water consumption was measured at the cage level (two mice per cage) and expressed as cumulative mL/mouse over each seven-day period. Data are presented as mean ± standard error of the mean (SEM; n = 4 cages per group). Statistical differences were assessed separately for each period using one-way analysis of variance (ANOVA), followed by Tukey's multiple-comparisons test; Figure S2: Genus-level differences in fecal microbiota before DSS-induced colitis. Relative abundances of selected bacterial genera at baseline (b) and after one week (1w) of dietary intervention in the CON, DSS, FRB, TRY, and FT groups. Boxplots show the distribution of relative abundances within each group. Differences among treatment groups were analyzed separately at each time point using the Kruskal–Wallis test, followed by Dunn's multiple-comparison test with Benjamini–Hochberg adjustment. Different lowercase letters indicate significant pairwise differences among treatments within the same time point ($p < 0.05$); groups sharing at least one letter are not significantly different. Kruskal–Wallis p values were adjusted across genera using the Benjamini–Hochberg procedure, with FDR-adjusted p values (q values) used to account for multiple testing; Figure S3: Family-level changes in fecal microbiota following dietary supplementation before DSS-induced colitis, Family-level differences in fecal microbiota before DSS-induced colitis. Relative abundances of selected bacterial family at baseline (b) and after one week (1w) of dietary intervention in the CON, DSS, FRB, TRY, and FT groups. Boxplots show the distribution of relative abundances within each group. Differences among treatment groups were analyzed separately at each time point using the Kruskal–Wallis test, followed by Dunn's multiple-comparison test with Benjamini–Hochberg adjustment. Different lowercase letters indicate significant pairwise differences among treatments within the same time point ($p < 0.05$); groups sharing at least one letter are not significantly different. Kruskal–Wallis p values were adjusted across genera using the Benjamini–Hochberg procedure, with FDR-adjusted p values (q values) used to account for multiple testing; Table S1: Pathogenic organism test; Table S2: Experimental diet composition; Table S3: Disease activity index (DAI) scoring criteria for DSS-induced colitis; Table S4: Nucleic acid concentration (ng/μL); Table S5: Primer sequences used for RT-qPCR analysis.

Author Contributions: Conceptualization, J.I., A.Z.A., Y.O. and H.S.; methodology, J.I., M.A., A.Z.A., Y.O. and H.S.; investigation, T.E.T., J.I., A.Z.A., M.F., F.S. and Y.O.; writing—original draft preparation, T.E.T. and J.I.; writing—review and editing, J.I., M.A., A.Z.A., H.-J.H., Y.O., Y.K. and H.S.; supervision, J.I., M.A., A.Z.A., H.-J.H., Y.O., Y.-L.C., W.-C.C., C.-L.Y., T.N., S.-C.Y., M.Z.H.H., Y.K. and H.S.; funding acquisition, A.Z.A. and H.S. All authors have read and agreed to the published version of the manuscript.

Funding: This research was partly supported by the JSPS RONPAKU (Dissertation Ph.D.) program to H.S., and the JSPS Grant-in-Aid for Early-Career Scientists (25K18187) to A.Z.A.

Institutional Review Board Statement: The study was conducted according to the guidelines of the Declaration of Helsinki and approved by the Animal Ethics Committee, Tohoku University (Sendai, Japan) (Approval No. 2019AgA-011-08 was granted on 13 Dember 2024).

Informed Consent Statement: Not applicable.

Data Availability Statement: The original contributions presented in this study are included in the article/Supplementary Materials. Further inquiries can be directed to the corresponding authors.

Acknowledgments: We acknowledge Animal Research Facility at the Graduate School of Agricultural Science, Tohoku University, for their technical support, and Habibul Bari Shozib, Senior Scientific Officer, Grain Quality and Nutrition Division, Bangladesh Rice Research Institute (BRRI), Bangladesh, for kindly providing us with the rice bran used in this study.

Conflicts of Interest: The authors declare no conflicts of interest.

Abbreviations

The following abbreviations are used in this manuscript:

ANOVA	One way analysis of variance
CLR	Centered log-ratio
DHGLUCONATE-PYR-CAT-PWY	Glucose degradation (oxidative)
FRB	Fermented rice bran
FDR	False discovery rate
FT	Fermented rice bran and tryptamine combination
GALACTARDEG-PWY	Galactose degradation
GLUCOSE1PMETAB-PWY	glucose-1-phosphate metabolism
HSD	Honestly significant difference
IBD	Inflammatory bowel disease
ILEUSYN-PWY	L-isoleucine biosynthesis
LDA	Linear discriminant analysis
LEfSe	Linear discriminant analysis effect size
Metacyc	Metabolic Encyclopedia
OR	Odd ratio
PCoA	Principal coordinate analysis
PERMANOVA	Permutational multivariate analysis of variance
PICRUSt2	Phylogenetic Investigation of Communities by Reconstruction of Unobserved States 2
PWY-2941	L-lysine biosynthesis
PWY-5743	3-hydroxypropanoate cycle (Autotrophic CO_2 fixation)
PWY-6944	Androstenedione degradation (Bacterial steroid catabolism)
PWY-7024	Super pathway of the 3-hydroxypropanoate cycle
PWY-7097	Vanillin and vanillate (lignin-derived aromatic compounds) degradation I
PWY-7098	Vanillin and vanillate degradation II
QIIME 2	Quantitative Insights into Microbial Ecology 2
SCFAs	Short-chain fatty acids
TRY	Tryptamine

References

1. Chang, J.T. Pathophysiology of Inflammatory Bowel Diseases. *N. Engl. J. Med.* **2020**, *383*, 2652–2664. [CrossRef] [PubMed]
2. Nishida, A.; Inoue, R.; Inatomi, O.; Bamba, S.; Naito, Y.; Andoh, A. Gut Microbiota in the Pathogenesis of Inflammatory Bowel Disease. *Clin. J. Gastroenterol.* **2018**, *11*, 1–10. [CrossRef] [PubMed]
3. Ruan, G.; Sun, Y.; Yu, Z.; Bai, X.; Yang, H.; Qian, J. Global, Regional, and National Burden of Inflammatory Bowel Disease from 1990 to 2021: Findings from the Global Burden of Disease 2021. *Gastroenterol. Rep.* **2025**, *13*, goaf082. [CrossRef] [PubMed]
4. Hracs, L.; Windsor, J.W.; Gorospe, J.; Cummings, M.; Coward, S.; Buie, M.J.; Quan, J.; Goddard, Q.; Caplan, L.; Markovinović, A.; et al. Global Evolution of Inflammatory Bowel Disease across Epidemiologic Stages. *Nature* **2025**, *642*, 458–466. [CrossRef] [PubMed]

5. Islam, J.; Koseki, T.; Watanabe, K.; Ardiansyah ; Budijanto, S.; Oikawa, A.; Alauddin, M.; Goto, T.; Aso, H.; Komai, M.; et al. Dietary Supplementation of Fermented Rice Bran Effectively Alleviates Dextran Sodium Sulfate-Induced Colitis in Mice. *Nutrients* **2017**, *9*, 747. [CrossRef] [PubMed]
6. Wee, V.T.K.; Shirakawa, H.; Yeh, S.-L.; Yeh, C.-L. Fermented Rice Bran Supplementation Attenuates Colonic Injury through Modulating Intestinal Aryl Hydrocarbon Receptor and Innate Lymphoid Cells in Mice with Dextran Sodium Sulfate-Induced Acute Colitis. *J. Nutr. Biochem.* **2024**, *123*, 109493. [CrossRef] [PubMed]
7. Elderman, M.; Hugenholtz, F.; Belzer, C.; Boekschoten, M.; van Beek, A.; de Haan, B.; Savelkoul, H.; de Vos, P.; Faas, M. Sex- and Strain-Dependent Differences in Mucosal Immunology and Microbiota Composition in Mice. *Biol. Sex Differ.* **2018**, *9*, 26. [CrossRef] [PubMed]
8. Zhao, Y.S.; Eweys, A.S.; Zhang, J.-Y.; Zhu, Y.; Bai, J.; Darwesh, O.M.; Zhang, H.-B.; Xiao, X. Fermentation Affects the Antioxidant Activity of Plant-Based Food Material through the Release and Production of Bioactive Components. *Antioxidants* **2021**, *10*, 2004. [CrossRef] [PubMed]
9. Kahlon, T. Rice Bran: Production, Composition, Functionality and Food Applications, Physiological Benefits. In *Fiber Ingredients*; Cho, S., Samuel, P., Eds.; CRC Press: Boca Raton, FL, USA, 2009. [CrossRef]
10. Agista, A.Z.; Rusbana, T.B.; Islam, J.; Ohsaki, Y.; Sultana, H.; Hirakawa, R.; Watanabe, K.; Nochi, T.; Ardiansyah; Budijanto, S.; et al. Fermented Rice Bran Supplementation Prevents the Development of Intestinal Fibrosis Due to DSS-Induced Inflammation in Mice. *Nutrients* **2021**, *13*, 1869. [CrossRef] [PubMed]
11. Tajasuwan, L.; Kettawan, A.; Rungruang, T.; Wunjuntuk, K.; Prombutara, P. Role of Dietary Defatted Rice Bran in the Modulation of Gut Microbiota in AOM/DSS-Induced Colitis-Associated Colorectal Cancer Rat Model. *Nutrients* **2023**, *15*, 1528. [CrossRef] [PubMed]
12. Shibayama, J.; Kuda, T.; Shikano, A.; Fukunaga, M.; Takahashi, H.; Kimura, B.; Ishizaki, S. Effects of Rice Bran and Fermented Rice Bran Suspensions on Caecal Microbiota in Dextran Sodium Sulphate-Induced Inflammatory Bowel Disease Model Mice. *Food Biosci.* **2018**, *25*, 8–14. [CrossRef]
13. Agus, A.; Clément, K.; Sokol, H. Gut Microbiota-Derived Metabolites as Central Regulators in Metabolic Disorders. *Gut* **2021**, *70*, 1174–1182. [CrossRef] [PubMed]
14. Roager, H.M.; Licht, T.R. Microbial Tryptophan Catabolites in Health and Disease. *Nat. Commun.* **2018**, *9*, 3294. [CrossRef] [PubMed]
15. Williams, B.B.; Van Benschoten, A.H.; Cimermancic, P.; Donia, M.S.; Zimmermann, M.; Taketani, M.; Ishihara, A.; Kashyap, P.C.; Fraser, J.S.; Fischbach, M.A. Discovery and Characterization of Gut Microbiota Decarboxylases That Can Produce the Neurotransmitter Tryptamine. *Cell Host Microbe* **2014**, *16*, 495–503. [CrossRef] [PubMed]
16. Islam, J.; Shirakawa, H.; Nguyen, T.K.; Aso, H.; Komai, M. Simultaneous Analysis of Serotonin, Tryptophan and Tryptamine Levels in Common Fresh Fruits and Vegetables in Japan Using Fluorescence HPLC. *Food Biosci.* **2016**, *13*, 56–59. [CrossRef]
17. Islam, J.; Sato, S.; Watanabe, K.; Watanabe, T.; Ardiansyah; Hirahara, K.; Aoyama, Y.; Tomita, S.; Aso, H.; Komai, M.; et al. Dietary Tryptophan Alleviates Dextran Sodium Sulfate-Induced Colitis through Aryl Hydrocarbon Receptor in Mice. *J. Nutr. Biochem.* **2017**, *42*, 43–50. [CrossRef] [PubMed]
18. Bhattarai, Y.; Williams, B.B.; Battaglioli, E.J.; Whitaker, W.R.; Till, L.; Grover, M.; Linden, D.R.; Akiba, Y.; Kandimalla, K.K.; Zachos, N.C.; et al. Gut Microbiota-Produced Tryptamine Activates an Epithelial G-Protein-Coupled Receptor to Increase Colonic Secretion. *Cell Host Microbe* **2018**, *23*, 775–785.e5. [CrossRef] [PubMed]
19. Zelante, T.; Iannitti, R.G.; Cunha, C.; De Luca, A.; Giovannini, G.; Pieraccini, G.; Zecchi, R.; D'Angelo, C.; Massi-Benedetti, C.; Fallarino, F.; et al. Tryptophan Catabolites from Microbiota Engage Aryl Hydrocarbon Receptor and Balance Mucosal Reactivity via Interleukin-22. *Immunity* **2013**, *39*, 372–385. [CrossRef] [PubMed]
20. Org, E.; Mehrabian, M.; Parks, B.W.; Shipkova, P.; Liu, X.; Drake, T.A.; Lusis, A.J. Sex Differences and Hormonal Effects on Gut Microbiota Composition in Mice. *Gut Microbes* **2016**, *7*, 313–322. [CrossRef] [PubMed]
21. Kader, M.A.; Biswas, P.S.; Aditya, T.L.; Anisuzzaman, M.; Hore, T.K.; Haq, M.E. Zinc Enriched High Yielding Rice Variety BRRI Dhan84 for Dry Season Rice Growing Areas of Bangladesh. *Asian Plant Res. J.* **2020**, *6*, 6–13. [CrossRef]
22. Sultana, A.; Amin, M.R.; Faruque, M.O.; Siddiquee, M.A.; Howlader, M.Z.H.; Alauddin, M. Fermented Rice Bran: A Promising Therapeutic Agent Against High-Fat Diet-Induced Metabolic Disorders. *Food Sci. Nutr.* **2026**, *14*, e71439. [CrossRef] [PubMed]
23. Gu, W.; Zhang, L.; Han, T.; Huang, H.; Chen, J. Dynamic Changes in Gut Microbiome of Ulcerative Colitis: Initial Study from Animal Model. *J. Inflamm. Res.* **2022**, *15*, 2631–2647. [CrossRef] [PubMed]
24. Usami, K.; Niimi, K.; Matsuo, A.; Suyama, Y.; Sakai, Y.; Sato, S.; Fujihashi, K.; Kiyono, H.; Uchino, S.; Furukawa, M.; et al. The Gut Microbiota Induces Peyer's-Patch-Dependent Secretion of Maternal IgA into Milk. *Cell Rep.* **2021**, *36*, 109655. [CrossRef] [PubMed]
25. Yagi, K. Assay for Blood Plasma or Serum. In *Methods in Enzymology*; Packer, L., Ed.; Academic Press: Orlando, FL, USA, 1984; Volume 105, pp. 328–331. [CrossRef] [PubMed]

26. Ohkawa, H.; Ohishi, N.; Yagi, K. Assay for Lipid Peroxides in Animal Tissues by Thiobarbituric Acid Reaction. *Anal. Biochem.* **1979**, *95*, 351–358. [CrossRef] [PubMed]
27. Islam, J.; Tanimizu, M.; Shimizu, Y.; Goto, Y.; Ohtani, N.; Sugiyama, K.; Tatezaki, E.; Sato, M.; Makino, E.; Shimada, T.; et al. Development of a Rational Framework for the Therapeutic Efficacy of Fecal Microbiota Transplantation for Calf Diarrhea Treatment. *Microbiome* **2022**, *10*, 31. [CrossRef] [PubMed]
28. Bolyen, E.; Rideout, J.R.; Dillon, M.R.; Bokulich, N.A.; Abnet, C.C.; Al-Ghalith, G.A.; Alexander, H.; Alm, E.J.; Arumugam, M.; Asnicar, F.; et al. Reproducible, Interactive, Scalable and Extensible Microbiome Data Science Using QIIME 2. *Nat. Biotechnol.* **2019**, *37*, 852–857. [CrossRef] [PubMed]
29. McDonald, D.; Jiang, Y.; Balaban, M.; Cantrell, K.; Zhu, Q.; Gonzalez, A.; Morton, J.T.; Nicolaou, G.; Parks, D.H.; Karst, S.M.; et al. Greengenes2 Unifies Microbial Data in a Single Reference Tree. *Nat. Biotechnol.* **2024**, *42*, 715–718. [CrossRef] [PubMed]
30. Lu, Y.; Zhou, G.; Ewald, J.; Pang, Z.; Shiri, T.; Xia, J. MicrobiomeAnalyst 2.0: Comprehensive Statistical, Functional and Integrative Analysis of Microbiome Data. *Nucleic Acids Res.* **2023**, *51*, W310–W318. [CrossRef] [PubMed]
31. Douglas, G.M.; Maffei, V.J.; Zaneveld, J.R.; Yurgel, S.N.; Brown, J.R.; Taylor, C.M.; Huttenhower, C.; Langille, M.G.I. PICRUSt2 for Prediction of Metagenome Functions. *Nat. Biotechnol.* **2020**, *38*, 685–688. [CrossRef] [PubMed]
32. Lloyd-Price, J.; Arze, C.; Ananthakrishnan, A.N.; Schirmer, M.; Avila-Pacheco, J.; Poon, T.W.; Andrews, E.; Ajami, N.J.; Bonham, K.S.; Brislawn, C.J.; et al. Multi-Omics of the Gut Microbial Ecosystem in Inflammatory Bowel Diseases. *Nature* **2019**, *569*, 655–662. [CrossRef] [PubMed]
33. Zuur, A.F.; Ieno, E.N.; Elphick, C.S. A Protocol for Data Exploration to Avoid Common Statistical Problems. *Methods Ecol. Evol.* **2010**, *1*, 3–14. [CrossRef]
34. Corthésy, B. Multi-faceted functions of secretory IgA at mucosal surfaces. *Front. Immunol.* **2013**, *4*, 185. [CrossRef] [PubMed]
35. Leeuwendaal, N.K.; Stanton, C.; O'Toole, P.W.; Beresford, T.P. Fermented Foods, Health and the Gut Microbiome. *Nutrients* **2022**, *14*, 1527. [CrossRef] [PubMed]
36. Salminen, S.; Collado, M.C.; Endo, A.; Hill, C.; Lebeer, S.; Quigley, E.M.M.; Sanders, M.E.; Shamir, R.; Swann, J.R.; Szajewska, H.; et al. The International Scientific Association of Probiotics and Prebiotics (ISAPP) Consensus Statement on the Definition and Scope of Postbiotics. *Nat. Rev. Gastroenterol. Hepatol.* **2021**, *18*, 649–667. [CrossRef] [PubMed]
37. Sommer, F.; Anderson, J.M.; Bharti, R.; Raes, J.; Rosenstiel, P. The Resilience of the Intestinal Microbiota Influences Health and Disease. *Nat. Rev. Microbiol.* **2017**, *15*, 630–638. [CrossRef] [PubMed]
38. Wastyk, H.C.; Fragiadakis, G.K.; Perelman, D.; Dahan, D.; Merrill, B.D.; Yu, F.B.; Topf, M.; Gonzalez, C.G.; Van Treuren, W.; Han, S.; et al. Gut-Microbiota-Targeted Diets Modulate Human Immune Status. *Cell* **2021**, *184*, 4137–4153.e14. [CrossRef] [PubMed]
39. Cassol, I.; Ibañez, M.; Bustamante, J.P. Key Features and Guidelines for the Application of Microbial Alpha Diversity Metrics. *Sci. Rep.* **2025**, *15*, 622. [CrossRef] [PubMed]
40. Shade, A. Drivers of Microbiome Biodiversity: A Review of General Rules, Feces, and Ignorance. *mBio* **2018**, *9*, e01294-18. [CrossRef] [PubMed]
41. Pabst, O.; Slack, E. IgA and the Intestinal Microbiota: The Importance of Being Specific. *Mucosal Immunol.* **2020**, *13*, 12–21. [CrossRef] [PubMed]
42. Bhattarai, Y.; Jie, S.; Linden, D.R.; Ghatak, S.; Mars, R.A.T.; Williams, B.B.; Pu, M.; Sonnenburg, J.L.; Fischbach, M.A.; Farrugia, G.; et al. Bacterially Derived Tryptamine Increases Mucus Release by Activating a Host Receptor in a Mouse Model of Inflammatory Bowel Disease. *iScience* **2020**, *23*, 101798. [CrossRef] [PubMed]
43. Kang, H.; Chen, Z.; Wang, B.; Chen, Z. The AhR/IL-22 Axis in Chronic Gut Inflammation: Unraveling Mechanisms and Therapeutic Prospects. *Front. Immunol.* **2025**, *16*, 1668173. [CrossRef] [PubMed]
44. Koropatkin, N.M.; Cameron, E.A.; Martens, E.C. How Glycan Metabolism Shapes the Human Gut Microbiota. *Nat. Rev. Microbiol.* **2012**, *10*, 323–335. [CrossRef] [PubMed]
45. Tanca, A.; Manghina, V.; Fraumene, C.; Palomba, A.; Abbondio, M.; Deligios, M.; Silverman, M.; Uzzau, S. Metaproteogenomics Reveals Taxonomic and Functional Changes between Cecal and Fecal Microbiota in Mouse. *Front. Microbiol.* **2017**, *8*, 391. [CrossRef] [PubMed]
46. Baldassano, S.N.; Bassett, D.S. Topological Distortion and Reorganized Modular Structure of Gut Microbial Co-Occurrence Networks in Inflammatory Bowel Disease. *Sci. Rep.* **2016**, *6*, 26087. [CrossRef] [PubMed]
47. Bian, X.; Wu, W.; Yang, L.; Lv, L.; Wang, Q.; Li, Y.; Ye, J.; Fang, D.; Wu, J.; Jiang, X.; et al. Administration of Akkermansia Muciniphila Ameliorates Dextran Sulfate Sodium-Induced Ulcerative Colitis in Mice. *Front. Microbiol.* **2019**, *10*, 2259. [CrossRef] [PubMed]
48. Ruan, G.; Chen, M.; Chen, L.; Xu, F.; Xiao, Z.; Yi, A.; Tian, Y.; Ping, Y.; Lv, L.; Cheng, Y.; et al. Roseburia Intestinalis and Its Metabolite Butyrate Inhibit Colitis and Upregulate TLR5 through the SP3 Signaling Pathway. *Nutrients* **2022**, *14*, 3041. [CrossRef] [PubMed]

49. Mohebali, N.; Weigel, M.; Hain, T.; Sütel, M.; Bull, J.; Kreikemeyer, B.; Breitrück, A. Faecalibacterium Prausnitzii, Bacteroides Faecis and Roseburia Intestinalis Attenuate Clinical Symptoms of Experimental Colitis by Regulating Treg/Th17 Cell Balance and Intestinal Barrier Integrity. *Biomed. Pharmacother.* **2023**, *167*, 115568. [CrossRef] [PubMed]
50. Koh, A.; De Vadder, F.; Kovatcheva-Datchary, P.; Bäckhed, F. From dietary fiber to host physiology: Short-chain fatty acids as key bacterial metabolites. *Cell* **2016**, *165*, 1332–1345. [CrossRef] [PubMed]
51. Parada Venegas, D.; De La Fuente, M.K.; Landskron, G.; González, M.J.; Quera, R.; Dijkstra, G.; Harmsen, H.J.M.; Faber, K.N.; Hermoso, M.A. Short chain fatty acids (SCFAs)-mediated gut epithelial and immune regulation and its relevance for inflammatory bowel diseases. *Front. Immunol.* **2019**, *10*, 277. [CrossRef] [PubMed]
52. Johnson, J.S.; Spakowicz, D.J.; Hong, B.-Y.; Petersen, L.M.; Demkowicz, P.; Chen, L.; Leopold, S.R.; Hanson, B.M.; Agresta, H.O.; Gerstein, M.; et al. Evaluation of 16S rRNA gene sequencing for species and strain-level microbiome analysis. *Nat. Commun.* **2019**, *10*, 5029. [CrossRef] [PubMed]

Disclaimer/Publisher's Note: The statements, opinions and data contained in all publications are solely those of the individual author(s) and contributor(s) and not of MDPI and/or the editor(s). MDPI and/or the editor(s) disclaim responsibility for any injury to people or property resulting from any ideas, methods, instructions or products referred to in the content.